GENERAL ELECTRIC

Research Laboratory

ADVANCES IN SOLID-STATE LUMINESCENCE

by

Ferd E. Williams

Report No. RL-805 February 1953

CLASS 1

SCHENECTADY, NEW YORK

CLASSES OF GENERAL ELECTRIC TECHNICAL REPORTS

CLASS 1: Available to anyone upon request.

CLASS 2: Available to G-E employees for use within the Company.

CLASS 3: Limited distribution within the Company.

Listed and abstracted in T. I. S. Briefs.

CLASS 4: Rigidly limited distribution within the Company. May not be sent outside the United States.

(Class 4 reports should be returned to Research Laboratory Publications if they are not needed.)

GENERAL ELECTRIC

Research Laboratory

REPORT NO. RL-805

ADVANCES IN SOLID-STATE LUMINESCENCE

Ferd E. Williams

February 1953

Published by
Research Publication Services
The Knolls
Schenectady, New York

FOR USE OF G-E EMPLOYEES ONLY

GENERAL ELECTRIC

Research Laboratory

SCHENECTADY, NEW YORK

TECHNICAL INFORMATION SERIES

Title Page

AUTHOR	SUBJECT CLASSIFICATION	NO.
Williams, Ferd E.	luminescence, solid-state	RL-805
		DATE: February 1953

TITLE

Advances in Solid-state Luminescence

52-605

ABSTRACT

Recent research on phosphors is reviewed with particular emphasis on the fundamental investigations of the mechanism of solid-state luminescence. The theoretical determination of the excitation and emission spectra of simple phosphors is described. Luminescent and trapping centers are identified. The phenomenon of electroluminescence is described and interpreted; and the preparation and properties of transparent cathode-ray tube screens are discussed.

G.E. CLASS	REPRODUCIBLE COPY FILED AT	NO. PAGES
1	Research Publication Services	37
GOV. CLASS.		

~~CONCLUSIONS~~

By cutting out this rectangle and folding on the center line, the above information can be fitted into a standard card file.

INFORMATION PREPARED FOR Light Production Studies Section, General Physics Research Department, Research Laboratory

TESTS MADE BY

COUNTERSIGNED DIV.

DIVISIONS LOCATION

FN-610-IM-RL (2-50)

TABLE OF CONTENTS

ADVANCES IN SOLID-STATE LUMINESCENCE*

Ferd E. Williams

I. INTRODUCTION

Solid-state luminescence is the branch of solid-state physics that is concerned with the phenomena associated with light emission from solids in excess of thermal radiation. Crystalline luminescent solids are commonly termed "phosphors." Their emission spectra are usually bell-shaped structureless bands at longer wave lengths than their absorption edge. Therefore, in contrast to incandescent bodies, phosphors are quite transparent to their own luminescent emission. Luminescence can be excited in many ways. Ultraviolet radiation, high-velocity electrons and nucleons, γ- and x-rays, and electric fields, excite suitable phosphors. The type or energy of excitation does not influence the emission spectra of most phosphors. The emission is characteristic of a particular impurity termed an "activator" in a particular valence state at a particular site in the lattice of the substance comprising the major part of the phosphor. For example, divalent manganese at zinc sites in zinc orthosilicate yields the typical green emission of willemite. When the excitation is removed, phosphors continue to emit their characteristic radiation for a finite time. Always, there is an initial exponential afterglow due to the short but finite lifetime of the emitting state of the activator. The time constant of this spontaneous afterglow varies from 10^{-6} second for zinc oxide to 10^{-1} second for manganese-activated zinc fluoride. In many cases, in addition, there is a long, hyperbolic afterglow that may persist for days. This component is often termed "phosphorescence" and is attributed in some phosphors to metastable states of the activator and, in others, to electron or hole traps remote from the activator ion. Phosphorescence is markedly dependent on temperature because thermal activation of the metastable activator or trap is prerequisite to emission; whereas the initial exponential afterglow is temperature-dependent only at temperatures high enough for radiationless de-excitation to become appreciable and the luminescent efficiency to be thereby reduced.

Phosphors are used primarily to convert electrical energy into light either for illumination--particularly fluorescent lighting; or for the visual display of information--television and radar. Phosphors are also used as x-ray, γ-ray, nucleon, and infrared detectors. Until quite

---

*Prepared as a chapter for Advances in Electronics, Volume V, Academic Press, New York (1953).

recently, luminescent solids were utilized exclusively in the form of microcrystalline powders.

In the fluorescent lamp, a complex doubly-activated calcium halophosphate phosphor converts the 2537 A radiation from the mercury discharge into visible radiation. The antimony activator provides the blue component of the white light; the manganese activator, the orange component. The phosphor powder, besides converting the ultraviolet to visible light, scatters the radiation diffusely. A theoretically more attractive method of utilizing phosphors for illumination is the direct conversion in the phosphor of electrical energy into luminescence. The possibility of a practical light source operating in this way has been enhanced by recent research on electroluminescence.

In the cathode-ray tube used in television, radar, and oscilloscopes, the sulfide and silicate phosphors convert the kinetic energy of the electrons into light. Silver-activated zinc sulfide and zinc-cadmium sulfide provide the blue and orange components of the conventional white television screen. The long persistent P-7 radar screen consists of a layer of silver-activated zinc sulfide, which converts the electron energy into blue light, and a layer of copper-activated zinc-cadmium sulfide, which converts the blue light into orange light with a phosphorescence not attainable by direct cathode-ray excitation. In cathode-ray tubes, the phosphor particles scatter the emitted radiation, thereby reducing the resolution and local contrast. In addition, scattering of the ambient illumination reduces the over-all contrast. The recent development of transparent phosphor films eliminates the limitations on contrast and resolution.

In the detection of fragments of nuclear processes, powdered phosphors have long been used. Rutherford, in performing his classical experiments on the scattering of α-particles by nuclei, observed visually on a sulfide phosphor screen the individual scintillations produced by single α-particles. Single-crystal phosphors combined with photomultiplier tubes now provide enormously more sensitive and convenient scintillation counters for nuclear research. Large single crystals of thallium-activated alkali halides are used in sensitive counters; whereas solid solutions of anthracene, napthalene, and terphenyl are used in very fast counters.

During recent years there have been important advances in many branches of solid-state physics. Phosphor research has undergone a transition from a strictly empirical technology to a fundamental science. Quantitative experimental and theoretical investigations on the simplest phosphors and the preparation of phosphors in the form of single crystals

and transparent films are responsible for the recent advances in solid-state luminescence. The advances in the detailed understanding of the mechanism of solid-state luminescence promise new applications for phosphors in electronic and illuminating devices.

II. THALLIUM-ACTIVATED POTASSIUM CHLORIDE

1. Identity of the Luminescent Center

Since the most recent reviews[1,2] of solid-state luminescence, the theory has advanced sufficiently to permit the fundamental calculation of the important properties of simple phosphors. In particular, the absorption and emission spectra of thallium-activated potassium chloride have been evaluated from first principles and the properties of the constituent ions. In addition, the principal electron traps of this phosphor have been identified as particular metastable states of the thallous ion.

The thallium-activated alkali halide phosphors consist of mixed crystals of thallous and alkali halides, with the thallous halide in dilute concentration. The thallous ions are distributed at random over alkali sites. Only thallous ions isolated from other thallous ions are effective activators. Therefore, as shown by Johnson and Williams,[3] if any one of the Z cation sites near a particular activator ion is occupied by another activator ion, the activation energy for radiationless de-excitation $E^{\ddagger}$ will be sufficiently reduced so that luminescence is quenched. The luminescent efficiency η is, consequently, the following function of gross activator concentration C:

$$\eta = \frac{C(1-C)^{Z}}{C+(\sigma/\sigma')\,(1-C)} \quad , \qquad (1)$$

where σ' and σ are the capture cross sections for the excitation energy of the activator ions and the nonactivator ions, respectively. Clearly, Z is dependent on temperature, and σ' and σ are dependent on wave length of excitation. Figure 1 shows that the emission at 3050 A of KCl:Tl with excitation in the 2460 A absorption band is in accord with Eq. (1), and that at 25° C occupancy of any one of the nearest 70 cation sites by another Tl^{+} quenches the luminescence of a particular Tl^{+}. It is, therefore, evident that the system responsible for the 2460 A excitation and the 3050 A emission band is an isolated Tl^{+} at a K^{+} site in KCl.

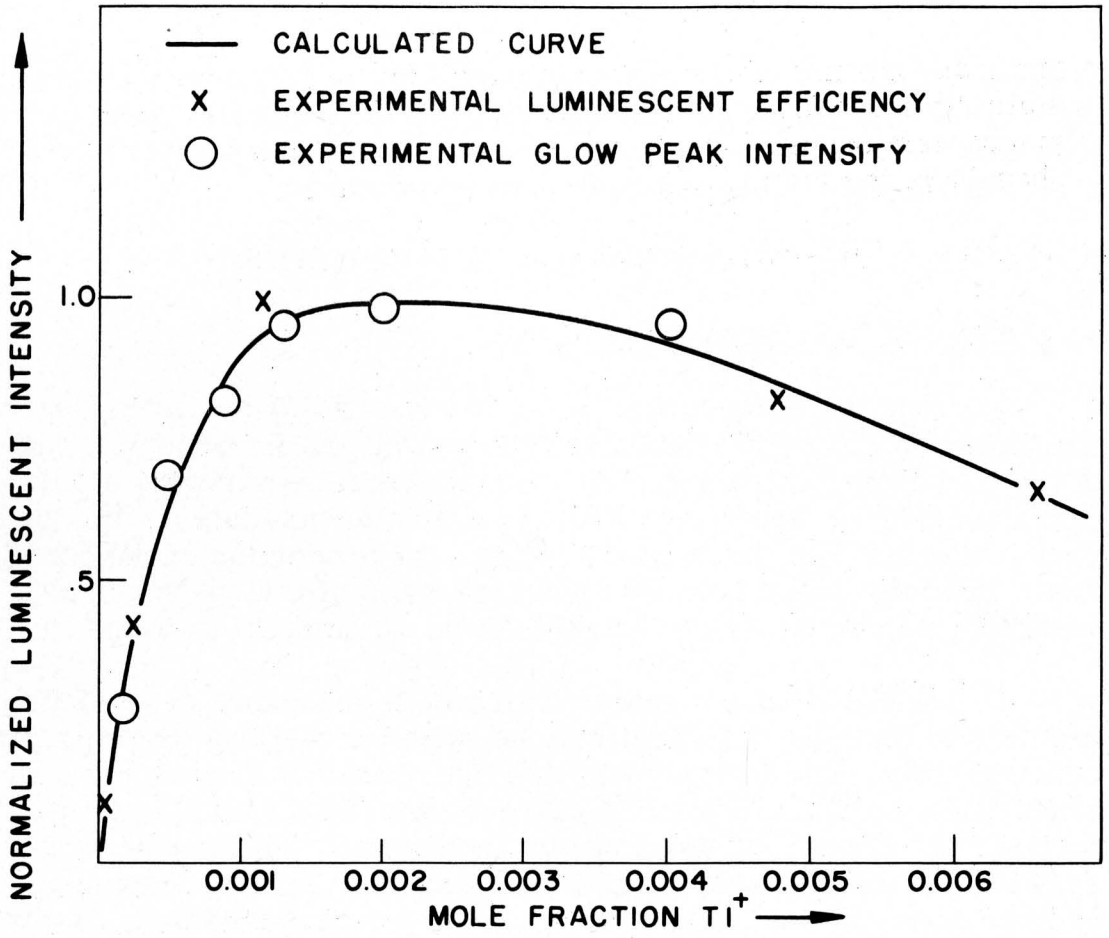

Fig. 1 Luminescent efficiency and thermoluminescent intensity versus activator concentration for KCl:Tl.

2. Energy Levels of the Luminescent Center

The atomic configuration of the luminescence center of KCl:Tl is shown in Fig. 2. The binding is ionic, as demonstrated by the success of Mayer[4] in evaluating the lattice energies of alkali and thallous halides from an ionic model. Seitz[5] concluded that the excited states of Tl^+, rather than electron transfer processes, are responsible for the excitation and emission bands of thallium-activated alkali halide phosphors. This conclusion is based primarily on the absence in these spectra of the doublet characteristic of the halide ions, the trivial dependence of peak positions on temperature, the close similarity in luminescent properties of phosphors containing different halides, and energy considerations. Williams[6] has computed the radial charge density of Tl^+ in the ground $^1S_0$ and the excited $^3P_1^o$ states by the Hartree self-consistent field method and found the outershell electrons of the free Tl^+

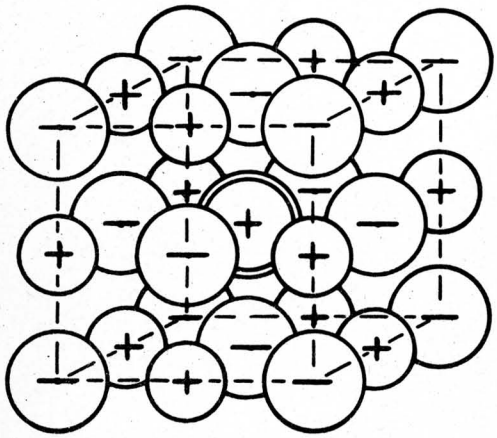

Fig. 2 Local environment of activator ion in alkali halide phosphors.

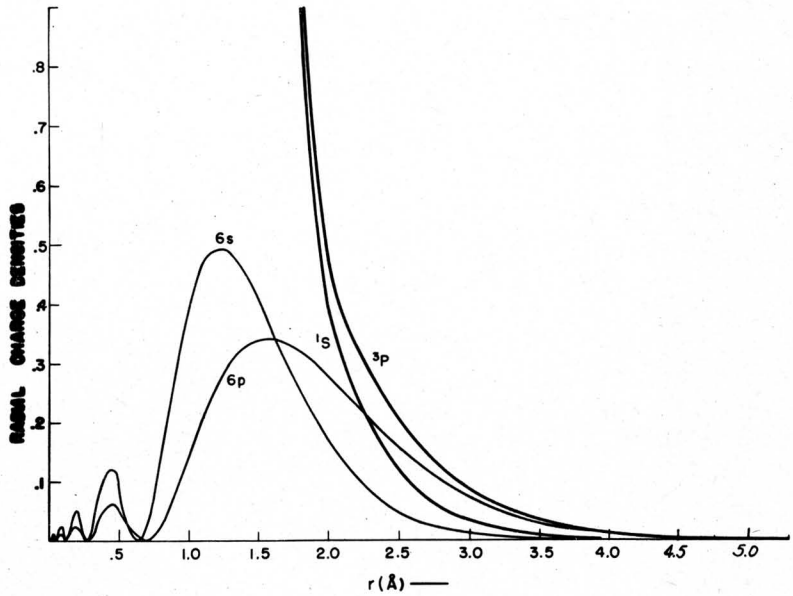

Fig. 3 Radial charge distribution of ^1S_o and $^3P_1^o$ Tl^+ and of the individual 6s and 6p electrons--Williams.[6]

in both states to be quite localized, as shown in Fig. 3. Therefore, even for the excited state of Tl^+, the ionic model is applicable. By calculating the change in lattice energies ΔE and $\Delta E'$ arising from substituting $^1S_o Tl^+$ and Tl^{++}, respectively, for K^+ in KCl, and by utilizing the following cycle, Johnson and Williams[7] computed the ground state of Tl^+ in KCl:Tl phosphor to be approximately 0.1 ev below the top of the filled band:

$$\begin{array}{ccc} Tl^+(g) + KCl(s) & \xrightarrow{I_2} & Tl^{++}(g) + KCl(s) + e \\ \downarrow \Delta E & & \downarrow \Delta E' - F \\ KCl{:}Tl^+(s) + K^+(g) & \xrightarrow{I_2^*} & KCl{:}Tl^{++}(s) + K^+(g) + e(s) \end{array} ,$$

where I_2 is the second ionization energy of Tl, F is the electron affinity of KCl in the lowest conduction state, and I_2^* is the ionization energy of Tl^+ in KCl and is, therefore, the energy from the $^1S_o Tl^+$ state to the conduction band. The band-theory model, including similar results for $^3P_1^o$ Tl^+, is shown in Fig. 4 for the equilibrium atomic configuration for $^1S_o Tl^+$. Since the excitation of KCl:Tl requires only 5 ev, it is deduced that in the emitting state the excited electron is bound to the activator by about 5 ev; therefore, highly localized wave functions and atomic rearrangements are involved. Also, the energy and probability of the $^1S_o \longrightarrow {}^3P_1^o$ transition are appropriate to the 2460 A absorption.

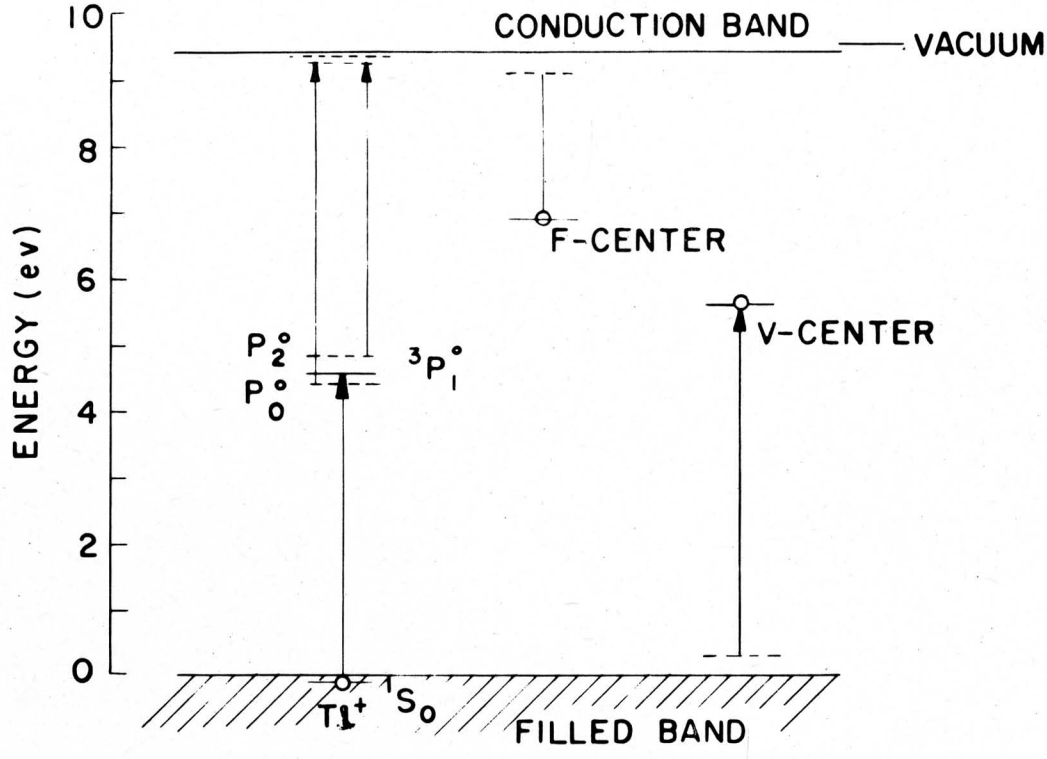

Fig. 4 Band-theory model of KCl:Tl--Johnson and Williams.[7]

3. Theory of Excitation and Emission Spectra

Following excitation, the activator ion is not in equilibrium with the lattice. The $^3P_1^o\,Tl^+$ interacts differently from the $^1S_0\,Tl^+$ with the six Cl^- shown in Fig. 2. The lifetime of the excited state is sufficiently long for equilibrium to be established with the neighbors displaced to new positions of minimum interaction energy. The polarizability and ionic radius of $^3P_1^o\,Tl^+$, and the exponential variation of repulsion energy and the coulomb overlap correction of $^3P_1^o\,Tl^+$ interacting with Cl^-, have been evaluated from the theoretical radial charge densities. For $^1S_0Tl^+$, these parameters are known experimentally, except for the coulomb overlap correction, which is negligible. By utilizing these parameters, the change in lattice energy can be computed for any atomic configuration of the unexcited or excited system. Madelung, exchange repulsion, van der Waals, ion-induced dipole, and coulomb overlap energies, are included. Only the interactions of the Tl^+ with the six Cl^- neighbors are peculiar to the state of the Tl^+; therefore, if the displacements are restricted to symmetric radial displacements of the six Cl^- and all other ions are displaced to positions of minimum potential energy, the

change in energy is a function of only one variable. In Fig. 5 is shown the resulting quantitative configuration coordinate model for $^1S_0$ and $^3P_1^o$ Tl^+. The configuration coordinate Δa is the displacement of the six Cl^- neighbors from the perfect KCl lattice sites. The curves are accurately parabolic.

The classical formula for the absorption or emission spectrum is:

$$P(\epsilon) = (Q/2\pi kT)^{1/2} e^{-Qq^2/2kT} (dq/d\epsilon) , \qquad (2)$$

where q is the displacement in the configuration coordinate from the minimum for the initial state, ϵ is the transition energy at q in accordance

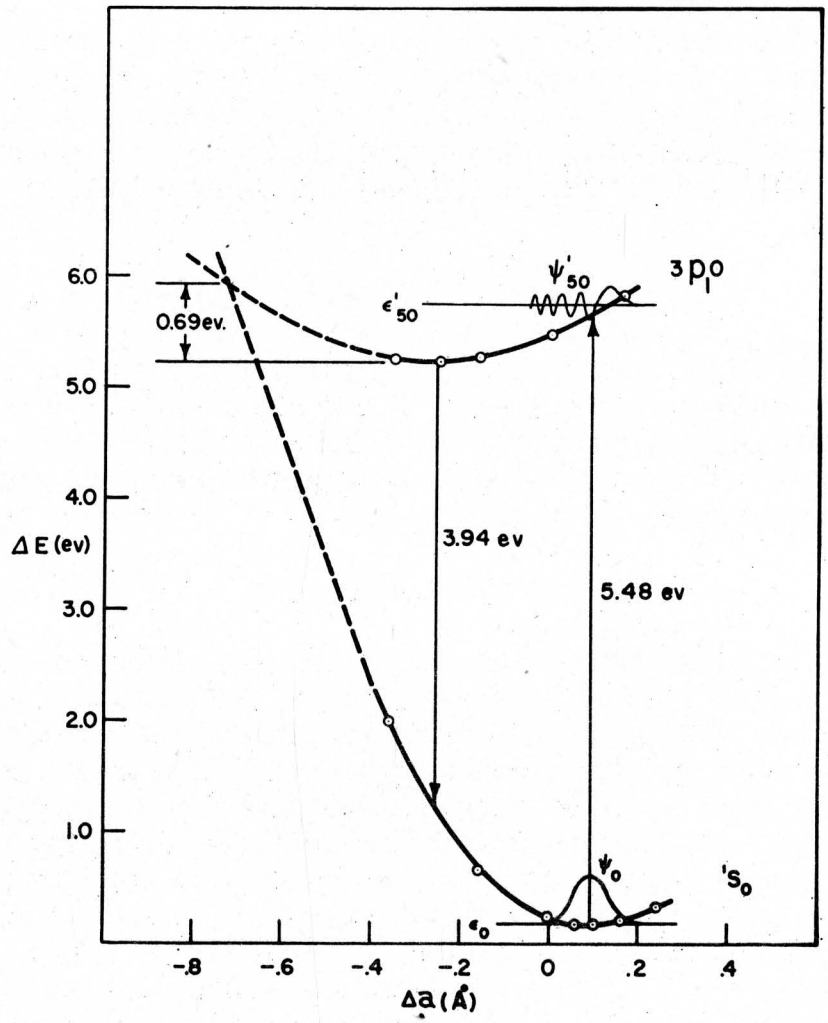

Fig. 5 Configuration coordinate model for $^1S_0$ and $^3P_1^o$ Tl^+ in KCl, including representative vibrational levels and wave functions--Williams and Hebb.[9]

with the Franck-Condon principle, and Q is the force constant for the initial state. In Fig. 6 are shown the theoretical and experimental absorption and emission spectra of KCl:Tl at 298°K. The agreement is satisfactory for both peak positions and half-widths. The Boltzmann factor in Eq. (2) produces a pronounced temperature-dependence of half-width for the absorption and emission spectra; and again in agreement with experiment, the half-widths are reduced a factor of two when the temperature is lowered to 80°K. It is concluded, therefore, that the $^1S_0 \rightleftarrows {}^3P_1^o$ transitions of Tl^+ are responsible for the 2460 A absorption and 3050 A emission bands.

4. Low-temperature Spectra

The quantum mechanical zero-point energy must be considered in deriving the spectra at very low temperatures.[8] Assuming that the normal modes of motion which involve appreciable changes in the potential energy of the activator system are approximated by an Einstein distribution, it is evident that the system is a harmonic oscillator with vibrational levels:

$$E_i = \hbar \, (Q/M)^{1/2} (i + \tfrac{1}{2}) \quad , \qquad (3)$$

where M is the effective mass of the six Cl^- coupled to the remainder of the lattice. With this model, the spectra will consist of a series of lines; however, in reality other neglected coordinates will broaden the lines. In KCl:Tl where no structure is observed, the theoretical spectra can be smoothed. The quantum mechanical spectrum is:

$$P(\epsilon_{if}) = N \, [\int \psi_i \psi_f dq \,]^2 \quad e^{-E_i/kT} \quad , \qquad (4)$$

where ϵ_{if} is the transition energy from the vibrational level i of the initial state to the level f of the final state, and ψ_i and ψ_f are, respectively, the vibrational wave functions of the initial and final levels. Williams and Hebb[9] have evaluated the absorption spectrum of KCl:Tl at 0°K by Eq. (4), approximating the exact ψ_f by the solution for a linear potential tangent to the parabola at q = 0. The theoretical half-width is in striking agreement with the absorption spectrum measured by Johnson and Studer[10] at 4°K. It is interesting that the most probable final vibrational levels are 41 for absorption and 67 for emission. In other words, following excitation ($^1S_0 Tl^+ \longrightarrow {}^3P_1{}^o Tl^+$), 41 phonons are dissipated as equilibrium is established with the activator in the excited state; and following emission ($^3P_1{}^o Tl^+ \longrightarrow {}^1S_0 Tl^+$), 67 phonons are dissipated.

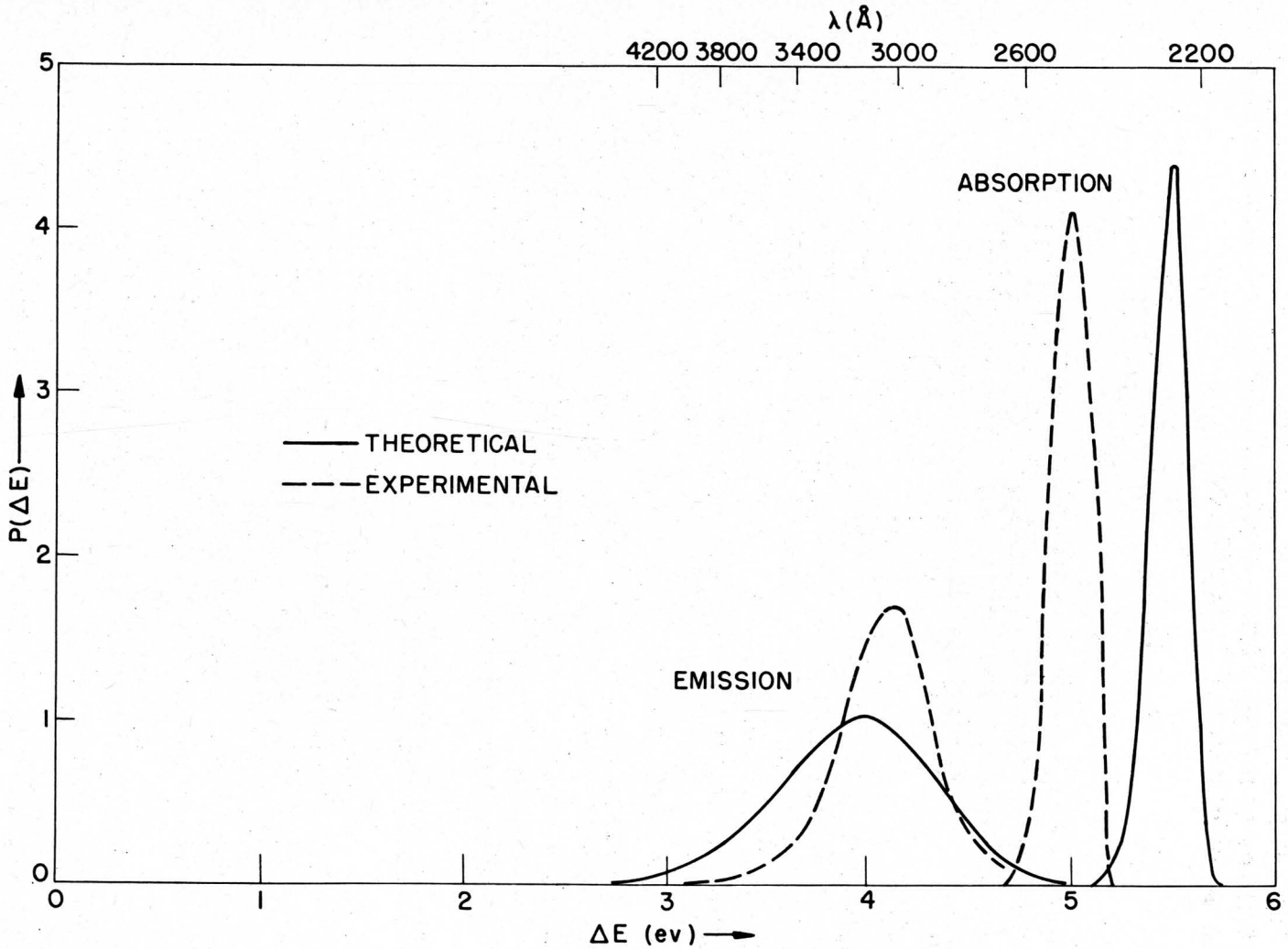

Fig. 6 Theoretical and experimental excitation and emission spectra of KCl:Tl--Williams.[6]

5. Radiationless De-excitation and Multiple Emitting States

The luminescent efficiency η as a function of temperature is determined by the ratio of the probability of emission A to the sum of the probabilities of all mechanisms of de-excitation, including the probability of radiationless de-excitation K'. Therefore:

$$\eta = \frac{A}{A+k'} = \frac{A}{A+se^{-E^{\ddagger}/kT}} \quad . \qquad (5)$$

The theoretical $E^{\ddagger}$ obtained from the intersection of the $^3P_1^o$ and ^1S_o states of Fig. 5 and the theoretical s obtained from the frequency of the harmonic oscillator model of the excited state are 0.69 ev and 2×10^{12} sec^{-1}, respectively. The corresponding experimental values are 0.60 ev and 10^{12} sec^{-1}.

Excitation of KCl:Tl at low temperatures in the 1960 A absorption band yields preferential emission at 4750 A. Energy and transition probability considerations identify these processes with the $^1S_o \rightleftarrows {}^1P_1^o$ transitions of isolated Tl^+. At higher temperatures, Johnson and Williams[11] have shown that a tendency toward equilibrium between the $^1P_1^o$ and $^3P_1^o$ states of the excited system is modified by emission. The configuration diagram of the $^1P_1^o$ state derived from absorption, emission, and equilibrium data is shown in Fig. 7. It is theoretically plausible that the equilibrium configuration of the $^1P_1^o$ Tl^+ has the $6Cl^-$ displaced inward because of the more extensive radial charge density of ^1P states compared to ^3P states, as shown by Hartree and Hartree,[12] and the consequent greater van der Waals and coulomb overlap interaction energies.

6. Electron Traps and Metastable States

More detailed information on the storage of excitation energy in phosphors can be obtained from thermoluminescent than from phosphorescent data. Thermoluminescence is measured by exciting the luminescent solid at a low temperature, removing the excitation and allowing phosphorescence to occur, and then heating the luminescent solid at a slow linear rate, simultaneously measuring emission intensity and temperature. A thermoluminescent curve with particularly well-resolved glow peaks is shown in Fig. 8. Each glow peak arises from thermally emptying an electron or hole trap having a particular energy depth.

With proper conditions of excitation, KCl:Tl exhibits eight individual glow peaks which can be separated by using slow heating rates; however, the two peaks shown in Fig. 8 are generally much more intense

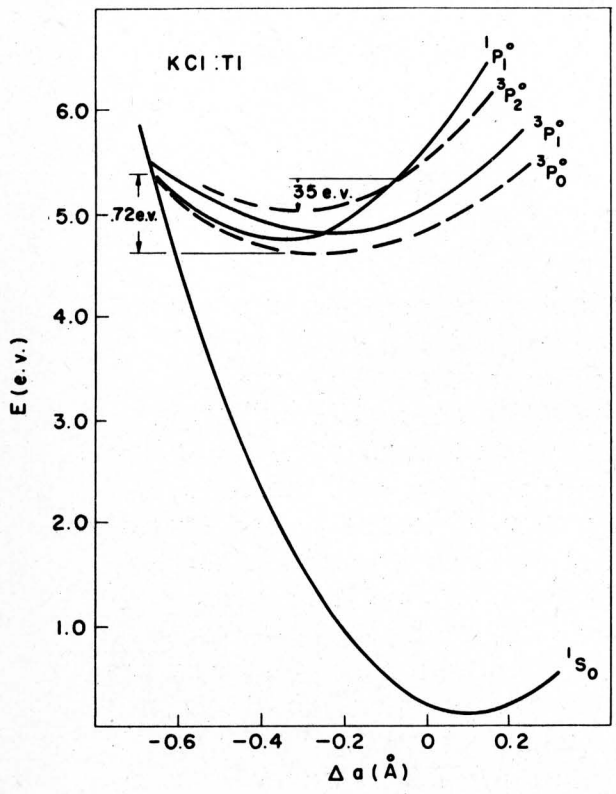

Fig. 7 Configuration coordinate model for ground state, emitting states, and trapping states of KCl:Tl--Johnson and Williams.(7)

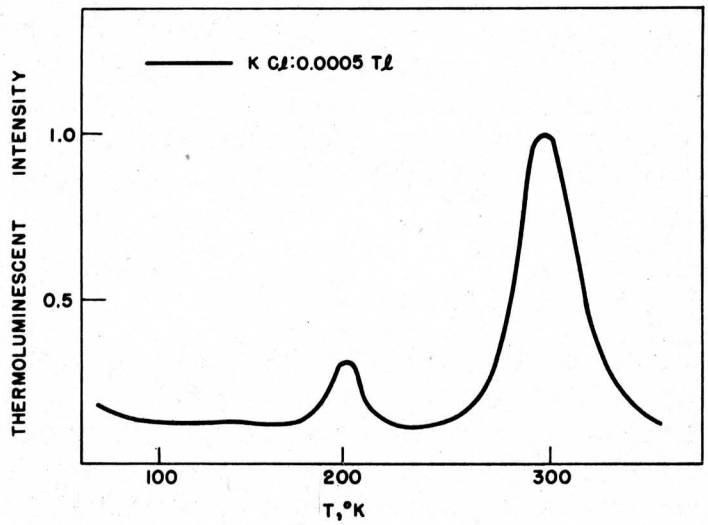

Fig. 8 Thermoluminescence of KCl:Tl--Johnson and Williams.(7)

than the others. The kinetics of themally emptying the two dominant traps accurately obeys the formula derived by Wilkins and Randall[13] for a first-order process with no retrapping:

$$J = -\frac{dn}{dt} = sn_o e^{-E_T^{\ddagger}/kT} \; e^{-\frac{s}{dT/dt}\int_o^T e^{-E_T^{\ddagger}/kT}\,dT}, \qquad (6)$$

where J and n are the luminescent intensity and concentration of occupied traps at the temperature T. The thermal trap depths E_T are 0.35 and 0.72 ev, and the frequency factors s are $10^8\ sec^{-1}$. Optically, the two dominant traps are preferentially emptied by 8000 A infrared radiation. In addition, Fig. 1 shows that the dependence of concentration of the 0.35-ev and 0.72-ev traps on thallium concentration is identical with the concentration dependence of luminescent efficiency. The increase in concentration of anion or cation vacancies by the addition of divalent impurities has no effect on the concentration of these traps. It is concluded from these experimental results and from Fig. 4 that the 0.35-ev and 0.72-ev traps are peculiar to the isolated Tl^+ responsible for emission and that they are localized states of Tl^+ differing in energy by a few tenths of an electron volt from the $^1P_1^o$ and $^3P_1^o$ emitting states. The metastable $^3P_0^o$ and $^3P_2^o$ states have these properties and are plotted in Fig. 7 so as to be in accord with the experimental thermal trap depths.

From transition probability considerations, it is evident that trapping occurs by excitation to the $^1P_1^o$ or $^3P_1^o$ state and then by transfer to the $^3P_0^o$ and $^3P_2^o$ states. Since the only activators that can participate in trapping are those excited to a sufficiently high vibrational level to permit passage over the potential barrier to the trapping states, the probability of trapping following initial excitation is of the form

$$\gamma = \gamma_o e^{-\epsilon^{\ddagger}/kT_{eff}}, \qquad (7)$$

where γ_o is determined by the lifetime of the higher vibrational levels and the frequency factor for transfer to the trapping states, $\epsilon^{\ddagger}$ is the activation energy for the system in the unexcited state to attain the critical configuration for subsequent trapping, and $T_{eff} = \theta \coth(\theta/T)$ and corrects for the quantum mechanical zero point energy $k\theta$.[9] The dependence on excitation temperature of the concentration of metastable activator ions and the rate and limiting concentration of metastable activator ions reveal that $\epsilon^{\ddagger}$ is 0.019 and 0.047 ev for the two dominant

traps of KCl:Tl and that the lifetimes of the higher vibrational levels are approximately equal to the period of vibration of the harmonic oscillator model, 10^{-12} second.

Incidentally, as expected from the band-theory model shown in Fig. 4, the metastable Tl^+ can be re-excited to higher electronic states, rendering feasible the formation of F- and V-centers. In fact, the concentration of traps simultaneously occupied is limited primarily by the re-excitation of metastable Tl^+.(7)

From the detailed theoretical treatment of KCl:Tl, it is clear that research on solid-state luminescence is entering into a period during which new luminescent phenomena will be predicted and phosphors will be designed and improved from fundamental considerations.

III. MANGANESE-ACTIVATED LUMINESCENT SOLIDS

1. Divalent Manganese-activated Phosphors

Divalent manganese is an effective activator in many diverse substances. Zinc orthosilicate activated with divalent manganese is the well-known P1 oscilloscope screen, and zinc-magnesium fluoride activated with divalent manganese is the P-12 radar screen. Divalent manganese is an activator in the calcium halophosphate fluorescent lamp phosphor. In addition, there exists a host of other luminescent solids activated with divalent manganese. These phosphors are characterized by single structureless emission bands, generally in the green, yellow, or red, and by exponential afterglow with a time constant of the order of milliseconds.

In this important class of phosphors, alkali halides activated with divalent manganese are the most amenable to theoretical study. The divalent manganese ions are distributed at random at the monovalent cation sites and an equivalent number of cation vacancies satisfy the charge requirements. Ionic diffusion measurements on alkali halides containing divalent cation impurities indicate that the divalent ion and the vacancy are not coupled. Therefore, the local atomic configuration is the same as shown in Fig. 2 except that a divalent ion is substituted at the center. Because of the divalency, the radial charge distribution of the Mn^{++} is even more localized than the charge distribution of Tl^+; therefore, the configuration coordinate model is even more applicable. The spherically symmetrical ground state ^6S Mn^{++} has the $1s^2 2s^2 2p^6 3s^2 3p^6 3d^5$ electronic configuration, with the $3d^5$ electrons having parallel spins.

A fundamental calculation of the absorption and emission spectra of KCl:Mn has recently been made by Williams.[14] As with the KCl:Tl, an electron transfer process does not lead to the observed characteristics. Excitation of the ^6S Mn^{++} to states having the electronic configurations .... $3d^4 4s$ and ....$3d^4 4p$ yields transition energies too large for the experimental excitation and emission energies. Excitation to states having the same principal and orbital quantum numbers for the individual electrons but having a change in multiplicity or electron spin were considered. The ^4P Mn^{++} having an electron configuration in which one of the $3d^5$ electrons has electron spin opposite to the other four was examined in detail. A Hartree-Fock calculation which includes the effect of exchange interactions between the 3d electrons was necessary to evaluate the radial charge densities of ^6S and ^4P Mn^{++}. The odd 3d electron of ^4P Mn^{++} has a more diffuse radial distribution because of the absence of exchange interaction with the other 3d electrons. The ^4P Mn^{++} is nonspherically symmetrical and can be oriented angularly to minimize the repulsion energy with the six Cl^- neighbors. From the quantitative potential energy curves for the ^6S and ^4P Mn^{++} systems, the theoretical excitation and emission spectra are evaluated and are found to be in satisfactory agreement with the experimental spectra.

Manganese-activated zinc fluoride has been extensively investigated in a series of fundamental experiments. Crawford and Williams[15] have shown from electrical measurements on single crystals that ZnF_2:Mn is an N-type impurity semiconductor; and Johnson and Williams[16,17] have shown from magnetic susceptibility measurements that the unexcited activator is in the ^6S Mn^{++} state, that the Mn^{++} are distributed at random over the Zn^{++} lattice sites, and that a decrease in multiplicity of approximately one Bohr magnetron per activator ion accompanies excitation. The concentration dependence of luminescent efficiency is described by Eq. (1), with Z equal to 22 at 25°C and equal to 13 at -193°C.[3] The low values of Z indicate a highly localized activator system. Optical absorption measurements by Parkinson and Williams[18] on evaporated ZnF_2, MnF_2, and ZnF_2:Mn films indicate that transitions of the Mn^{++} are responsible for the efficient optical excitation of this phosphor. The photoconductivity of ZnF_2 :Mn is quite independent of the luminescence. Thermoluminescent measurements were made by J. S. Johnson and Williams[19] to investigate electron trapping in ZnF_2 :Mn. The composite glow curve is shown in Fig. 9. Equation (6) for the first-order mechanism is found to fit the individual glow peaks rather well; however, a correction for some retrapping improves the agreement with experiment. The thermal trap depths are shown in Fig. 9; the frequency factors for untrapping are approximately the theoretical value kT/h for all traps.

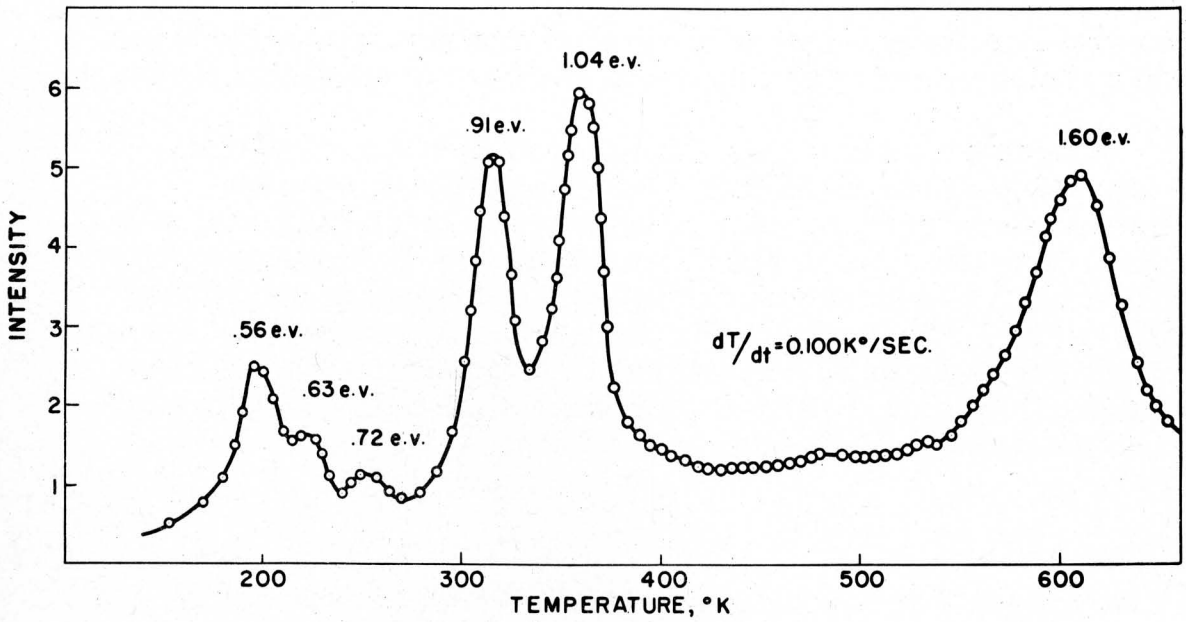

Fig. 9 Thermoluminescence of ZnF_2:Mn.

The experimental observations on ZnF_2:Mn relating to excitation and emission are obviously in accord with these transitions occurring between the ^6S and ^4P states of isolated Mn^{++}. The precise identification of the electron or hole traps in ZnF_2:Mn awaits further experimental and theoretical studies.

Multiple emission bands are encountered in silicate and germanate phosphors activated with divalent manganese. For example, willemite with high manganese content at low temperatures exhibits a red emission band in addition to the normal green band. To explain the multiple emission band, a "cluster theory" and a "coordination theory" have been proposed. According to the cluster theory, the relative intensities of the individual emission bands are attributed to the interaction between manganese ions affecting the lifetimes of various excited states. According to the coordination theory, the different emission bands are attributed to manganese ions at cation sites having different numbers of nearest neighbors. Kröger and Zalm[20] have recently reviewed these theories, and have analyzed data on the temperature-dependence and dependence on manganese concentration of the intensities of the multiple bands. They conclude that the cluster theory provides the simpler interpretation.

2. Tetravalent Manganese-activated Phosphors

In addition to the large number of inorganic phosphors activated with divalent manganese, there exist several luminescent solids activated

with tetravalent manganese. The tetravalent manganese-activated phosphors are characterized by red emission having an unusual fine structure.

Extending the earlier work of Tiede and Villain,[21] Kröger[22] has proven by chemical methods that the activator in manganese-activated magnesium orthotitanate prepared in an oxidizing atmosphere is tetravalent manganese. Kröger, Hoogenstraaten, Bottema, and Botden[23] have shown that the temperature-dependence of luminescent efficiency of $Mg_2TiO_4:Mn^{++++}$ is in accord with Eq. (5) and that the probabilities of emission and of radiationless de-excitation dominate the temperature-dependence of afterglow as well as efficiency. The initial exponential afterglow constant α is, therefore, of the form:

$$\alpha = A + se^{-E^{\ddagger}/kT} . \qquad (8)$$

Kröger and van den Boomgaard[24] have also shown by chemical methods that the emission of manganese-activated magnesium orthogermanate prepared with excess magnesium oxide is due to manganese in a valence state greater than two, rather than to divalent manganese as assumed by Patten and Williams.[25] Concurrently, Thorington[26] recognized that the activator is most probably tetravalent manganese and discovered that the peak luminescent efficiency of this phosphor is at 350°C. The emission spectrum is shown in Fig. 10.

Prener[27] recently reported luminescence characteristic of tetravalent manganese in magnesium oxide. The preparation must be accomplished in an oxygen atmosphere and monovalent lithium must be added in order for the Mn^{++++} to be formed and to enter the MgO lattice. X-ray data is in accord with the Li^+ and the Mn^{++++} substituting at Mg^{++} sites in the MgO rocksalt structure. Chemical analysis indicates for the manganese an average oxidation state of 3.5, whereas paramagnetic resonance measurements by Hershberger and Leifer[28] indicate an average valence of 3.8. The simple $MgO:Mn^{++++}$, Li^+ should be amenable to quantitative theoretical analysis.

Various proposals have been made regarding the origin of the fine structure of emission of luminescent solids activated with tetravalent manganese. Splitting of energy levels of the free activator ion by the crystal field and the multiplet structure of the free activator ion have been proposed. Patten and Williams[25] have shown that the dependence on temperature of the intensities of the individual emission bands of the germanate is in accord with a Boltzmann distribution among sublevels of the emitting state. Kröger and van den Boomgaard[24]

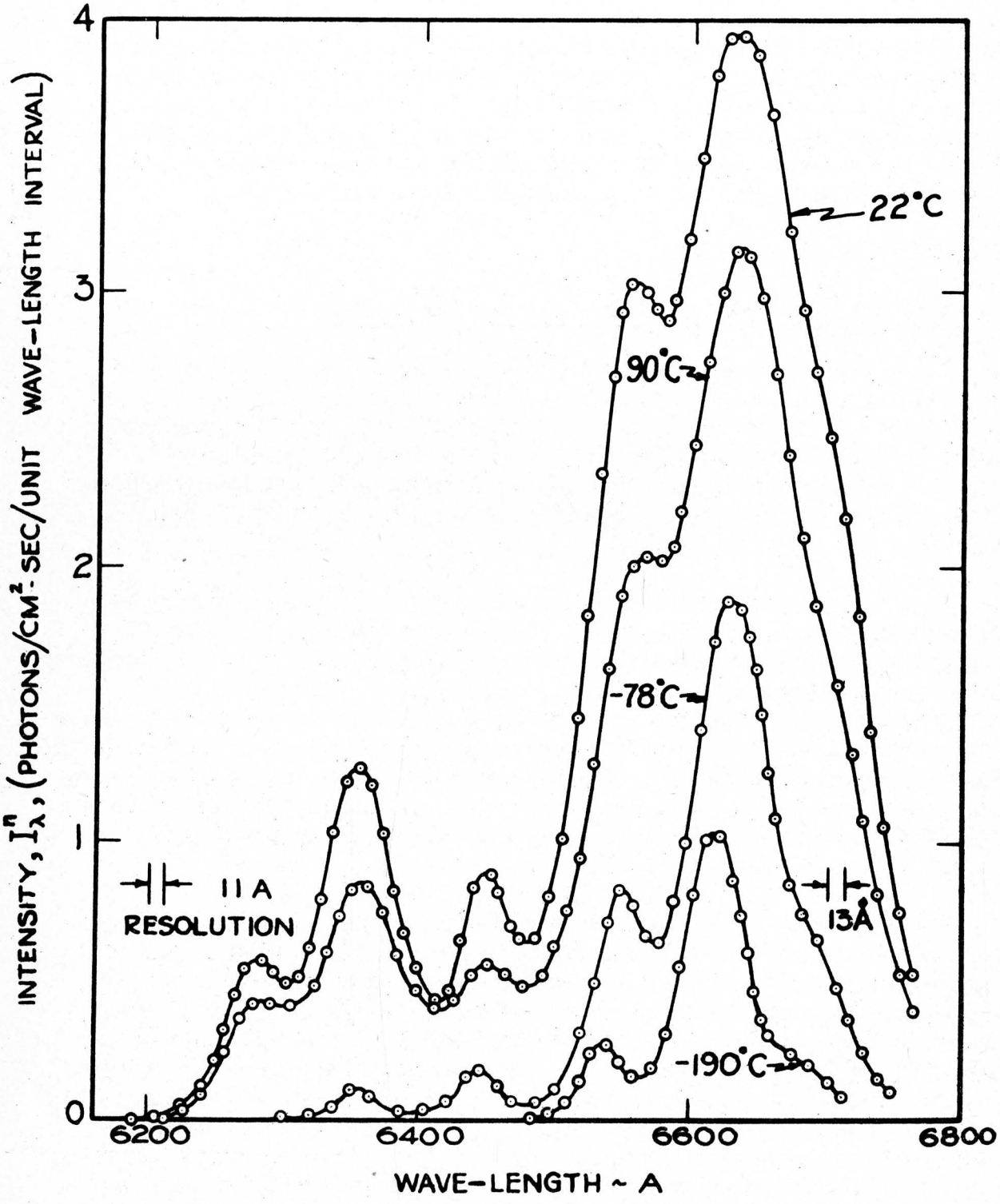

Fig. 10 Emission spectrum of $4MgO \cdot GeO_2$:Mn--Patten and Williams.(25)

have generalized the analysis to include the effect of nonradiative as well as radiative transitions. It appears probable that the sublevels are the vibrational fine structure predicted by Eq. (4). The activator system in tetravalent manganese phosphor is extremely localized, so that only a single configuration coordinate is significant and other atomic coordinates do not appreciably broaden the vibrational fine structure.

IV. SULFIDE PHOSPHORS

1. Tentative Identification of the Luminescent Centers

The zinc sulfide and zinc-cadmium sulfide phosphors provide the bulk of the cathode-ray tube screens for television and radar. Self-activated or activated with silver or copper, this class of luminescent solids is characterized by efficient excitation by 3650 A radiation or cathode rays; by broad, structureless emission bands; and by hyperbolic afterglow which is markedly dependent on temperature and intensity of excitation.

The optimum activator concentration for sulfide phosphors is approximately 0.01 mole per cent. The luminescent efficiency as a function of activator concentration is given by Eq. (1), with Z very large. For ZnS:Cu, Z equals 4000. In other words, the excited luminescent centers of sulfide phosphors are spacially quite extensive and the emitting state of the activator system is near the lower edge of the conduction band. The configuration coordinate calculations based on the use of unperturbed atomic wave functions as applied to the thallium and manganese localized activator systems are obviously not applicable to the activator systems of sulfide phosphors.

Until quite recently, interstitial zinc, copper, and silver atoms were considered to be the luminescent centers in self-activated and in copper- and silver-activated zinc and zinc-cadmium sulfide phosphors. Kröger, Hellingman, and Smit[29] prepared ZnS:Cu in controlled atmospheres of H_2S and HCl vapors and showed that Cl^- enters the phosphor lattice in amounts equivalent to the concentration of luminescent centers. The intensities of the green and blue bands of ZnS:Cu were found to depend on the composition of the H_2S-HCl atmosphere. They explained their results qualitatively by assuming that the green-emitting luminescent centers are formed when copper is incorporated in ZnS as CuCl, whereas the blue-emitting luminescent centers are formed when copper dissolves as Cu_2Cl. Blue-emitting centers characteristic of self-activated ZnS are formed by incorporation of Cl^- with simultaneous

reduction of Zn^{++} to Zn^{+}. Incidentally, a halide salt is invariably used as a flux in preparing sulfide phosphors. Similarly, Kröger and Dikhoff[30] showed that AgCl and AuCl enter the lattice when ZnS:Ag and ZnS:Au are prepared. Trivalent ions such as Al^{+++} were also found to facilitate the introduction into the lattice of the copper, silver, and gold luminescent centers. The activation of sulfide phosphors is clearly governed by charge compensation. In order for the monovalent cations to substitute at Zn^{++} sites in ZnS, an equivalent concentration of monovalent anions must substitute at $S^{=}$ sites or an equivalent concentration of trivalent cations must substitute at Zn^{++} sites. The emission spectra of Zn^{+}, Cu^{+}, Ag^{+}, or Au^{+} activated ZnS are found to depend on the monovalent cation and not on the monovalent anion or trivalent cation; therefore, the monovalent cation surrounded by four sulfur ions is probably the luminescent center in these phosphors. The identification of the luminescent center of blue-emitting ZnS:Cu as Cu_2^{+} is somewhat more tenuous. In support of these conclusions, Kröger and Smit[31] have made a quantitative analysis of the dependence of the formation of luminescent centers on the composition of the H_2S-HCl atmosphere during preparation.

2. Energy Levels of the Luminescent Centers

The luminescence of ZnS:Ag, ZnS:Au, ZnS:Cu, and ZnS:Zn is due to an electronic transition between an energy level close to the lower edge of the conduction band and an energy level above the filled band. The energy of the ground state of the luminescent center depends on the identity of the activator. The corresponding (Zn,Cd)S phosphors have the fundamental absorption edge and the luminescent emission spectra shifted equally to longer wave lengths. It appears, therefore, that the energy separation of the ground state of the luminescent center and the filled band is independent of cadmium substitution. On this basis, Klasens[30] suggested that the ground state of the luminescent center is a level due to sulfur ions, perturbed by an activator ion at an adjacent site. Classically, the filled band can be considered as sulfur ion levels. The presence of an adjacent monovalent cation at a Zn^{++} site obviously reduces the binding energy of the electrons of the $S^{=}$; therefore, a discrete state exists above the filled band and is bound to the monovalent cation. The exact energy of the ground level of the activator system obviously depends on the polarization, van der Waals, and exchange interactions of the activator ion with the adjacent sulfur ions.

It has already been emphasized that the spatial extension of the excited luminescent center is large compared to the lattice constant of ZnS. The coulomb field of the ionized center determines the binding energy. The ionization energy of the excited center is given by the Bohr formula:

$$E_I = 2\pi m^* e^4/K^2h^2 \quad , \qquad (9)$$

where K is the dielectric constant of ZnS. Substituting the electron mass for the effective mass m^*, E_I is approximately 0.2 ev. Roberts and Williams[32] in a general theoretical treatment of the nonlinear luminescence of sulfide phosphors computed the emitting state of the $Zn_{0.5}Cd_{0.5}S$:Ag, Ni phosphor as 0.17 ev below the conduction band. Their complete band-theory model is shown in Fig. 11 for the luminescent center in the equilibrium atomic configuration of the emitting state.

3. Electron and Positive Hole Traps

The identity of the traps responsible for the temperature- and intensity-dependent hyperbolic afterglow of sulfide phosphor has not been established. The breadths and number of the glow peaks observed in thermoluminescent experiments suggest that many discrete traps with different thermal depths or a continuous energy distribution of traps are present. The small energy difference between the emitting state of the luminescent center and the conduction band permits thermal ionization. Migration of the conduction electron to electron traps distant from the luminescent center is then feasible. In addition, the ionized luminescent center can be thermally excited to yield a positive hole in the filled band, and migration to a positive hole trap may occur. Thermal excitation of the trapped electron and trapped hole are then prerequisite to luminescent emission.

Wise[33] has recently proposed an ingenious theory of traps in sulfide phosphors. He proposes that the electron traps that dominate phosphorescence and thermoluminescence are various states of the luminescent center. The deep traps are simply ionized luminescent centers, and the trapped state of the electron is a metastable state of the luminescent center. This is the same as the metastable states of thallium-activated alkali halides, except that in the sulfide phosphors the conduction band may be utilized in the transition from the emitting state to the metastable state. In addition, Wise proposes that the ionized center which has trapped an electron can trap a second electron. This is similar to the acceptance of a second electron by an F center, which is an

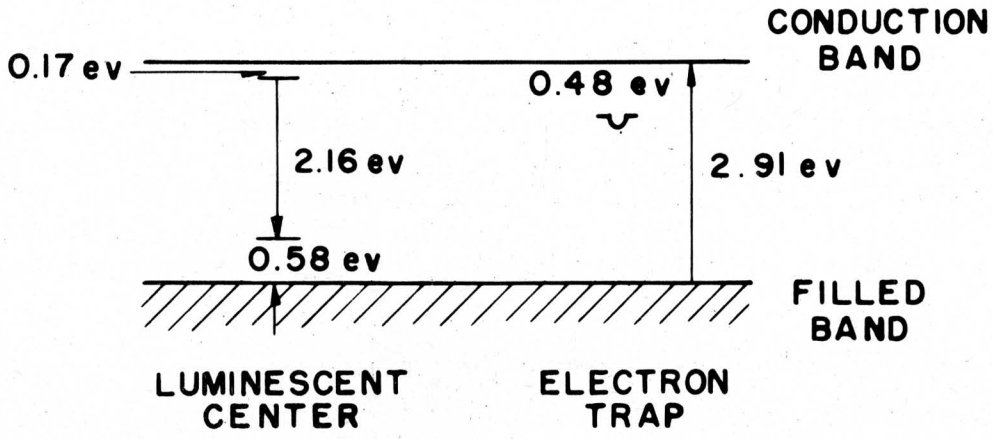

Fig. 11 Band-theory model of ZnS·CdS:Ag,Ni for the equilibrium configuration of the emitting state.

electron trapped at a halide vacancy in an alkali halide. The F center thereby becomes an F' center. It can be shown that the effective trap depth decreases as the concentration of metastable luminescent centers increases.

Additional experimental and theoretical work is necessary for the unambiguous identification of the traps in sulfide phosphors.

V. ELECTROLUMINESCENCE

1. Introduction to Electroluminescence

A fundamentally attractive method of producing light, both for illumination and for the visual display of information, is to directly convert in a semiconducting solid electrical energy into luminescence. The excitation of luminescence by the application of an electrical potential to a phosphor crystal or to a suspension of phosphor crystals is termed "electroluminescence." There have recently been several significant experimental advances in the field. In addition, two theoretically sound mechanisms for the phenomenon of electroluminescence have been proposed.

Destriau[34] discovered and extensively studied the electroluminescence of sulfide phosphors. An a-c electrical potential was applied to a suspension of phosphor particles in a liquid between two plane parallel electrodes. With this excitation, the brightest phosphor--copper-activated zinc sulfide prepared in the conventional way--is still too feeble for a practical light source. Payne, Mager, and Jerome[35] have reported electroluminescent cells having improved performance.

The excitation by an applied potential of light emission from silicon carbide crystals was earlier investigated by Lossew.[36] Either an a-c or d-c electrical potential is applied with point contact electrodes directly to a silicon carbide crystal. The light emission is localized to regions near the anode and cathode, and is again quite feeble. Tetzner[37] demonstrated that the emission at the cathode is solid-state luminescence.

2. Phosphor-dielectric Electroluminescent Cells

Roberts[38] has recently made quantitative measurements and calculations on improved electroluminescent cells. The cells are constructed by dispersing a copper-activated zinc sulfoselenide phosphor powder in a thermoplastic dielectric matrix and forming the mixture in uniform sheets of accurately known thickness. Conducting glass and aluminum foil are applied intimately to opposite sides of the sheets, and dielectric constant and dielectric loss measurements made. Approximating the phosphor particles by homogeneous spheres, Roberts has derived from electromagnetic theory and the theorem of Clausius and Mosotti the following equation for the local field in the phosphor E_2 in terms of the applied field E, the dielectric constants of the matrix K_1 and of the phosphor K_2, and the volume fraction of phosphor V_2:

$$\frac{E_2}{E} = \frac{3K_1}{2K_1 + K_2 - V_2(K_2 - K_1)} \quad . \qquad (10)$$

From the data on cells prepared with various matrixes having markedly different dielectric constants, he proved that the brightness of electroluminescence depends only on the local electric field in the phosphor. Figure 12 shows the brightness versus local field for several dielectrics. The theoretical brightness versus dielectric constant of the matrix is shown in Fig. 13. The temperature-dependence of electroluminescence was measured from -100°C to +50°C on a polystyrene cell. Polystyrene was selected because its dielectric constant is quite independent of temperature in this temperature range. The electroluminescent brightness versus temperature shown in Fig. 14 is sufficiently constant to indicate that thermal activation does not play a significant role in the electroluminescence of sulfide phosphors.

3. Impact Excitation Mechanism

Piper and Williams[39] have recently studied electroluminescence in single crystals of copper-activated zinc sulfide. Quantitative measurements on the single crystals, interpreted theoretically, have revealed the mechanism of electroluminescence of sulfide phosphors.

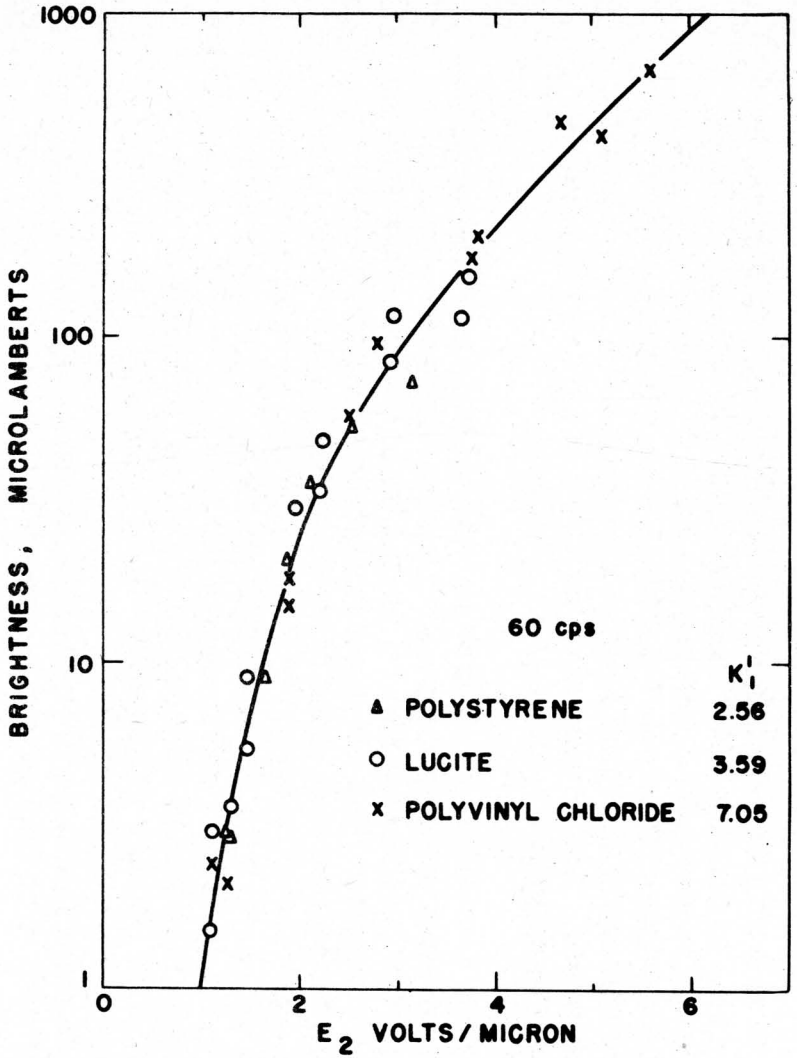

Fig. 12 Electroluminescent brightness versus local electric field--Roberts.(38)

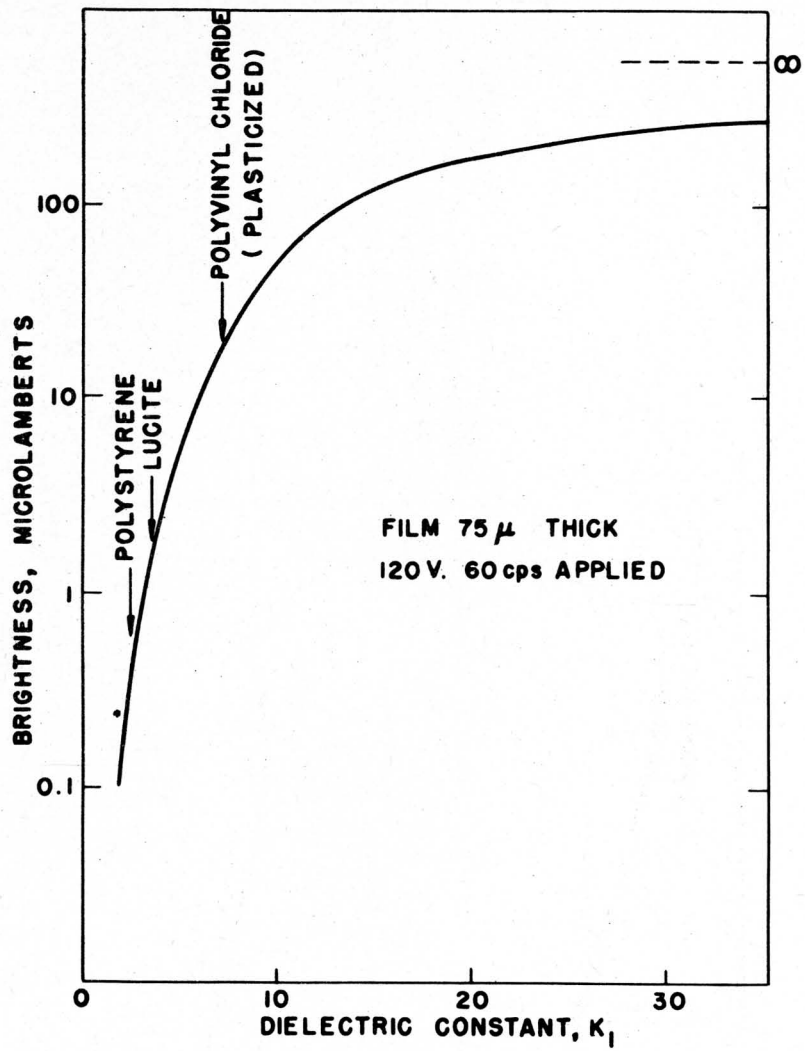

Fig. 13 Electroluminescent brightness versus dielectric constant of dielectric matrix--Roberts.(38)

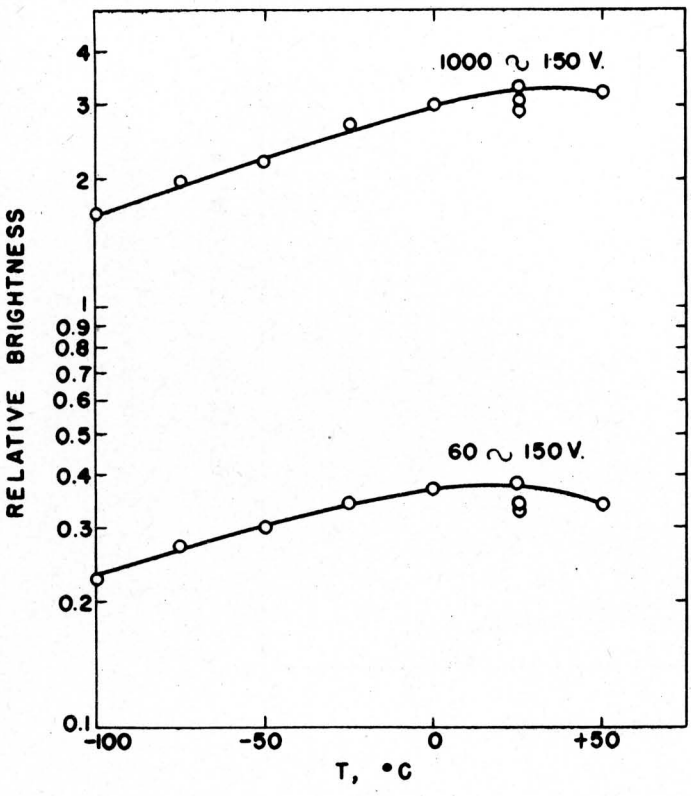

Fig. 14 Electroluminescent brightness versus temperature for powdered phosphor-dielectric cell--Roberts.(38)

The zinc sulfide crystals are grown from the vapor phase by sublimation in a vacuum at 1090°C, as described by Piper.(40) Both unactivated and copper-activated crystals were prepared. The unactivated crystals exhibit intrinsic electrical conductivity above 200°C, thereby demonstrating normal semiconducting behavior for a highly purified substance. The copper-activated zinc sulfide crystals luminesce upon the application of a-c or d-c voltages.

With a d-c voltage applied to a ZnS:Cu single crystal clamped between metal electrodes, the current increases exponentially with voltage, reversibly to breakdown. The nonohmic behavior suggests the presence of a barrier. The electroluminescent emission intensity is proportional to the current. With different metals used for the two electrodes, the current-voltage or brightness-voltage characteristic is found to be characteristic of the cathode material. The presence of a cathode barrier is further confirmed by the pronounced photoconductivity observed when the cathode side of the crystal is irradiated with ultraviolet. Since the barrier is dependent on the cathode material, it is probably of the Mott-Schottky(41,42) exhaustion type, arising from the difference in work functions of the semiconducting zinc sulfide and the metal electrode. The applied d-c voltage is obviously not uniformly

distributed across the single crystal but is almost entirely across the barrier. Assuming a reasonable barrier height and donor concentration, quantum mechanical tunneling through the barrier occurs with the applied voltages necessary for d-c electroluminescence of ZnS:Cu. With an applied potential of 10^3 volts, the local field at the cathode surface is 10^7 v/cm. This field is an order of magnitude greater than the field necessary for electrons to be accelerated in the conduction band faster than they are decelerated by interaction with the lattice; therefore, the electrons that penetrate the barrier will be accelerated to kinetic energies sufficient for impact excitations of the activator ions. In other words, local electronic breakdown occurs; however, avalanches are probably not formed, since the high field region is limited to the barrier thickness of the order of 10^{-4} cm. The final impact excitation process is similar to the excitation of the phosphor by cathode rays.

With an a-c voltage applied to ZnS:Cu single crystals, Piper and Williams report and interpret two distinct components of electroluminescence. The two components were resolved by observing on an oscilloscope the light output as a function of the voltage cycle as shown in Fig. 15. The pulse widths in electrical degrees do not change appreciably from 60 to 6000 cps. Depending on the magnitude of the applied voltage, either light pulses in phase with the voltage or light pulses out of phase with the voltage dominate the electroluminescence.

The in-phase component appears at a high critical voltage and increases rapidly in intensity with further increase in voltage. The critical voltage is dependent on the electrode material. Electrodes of high work function, such as platinum, exhibit a higher threshold voltage than electrodes of low work function, such as aluminum. With different metals used for the two electrodes, the in-phase pulse characteristic of a particular electrode material appears when that electrode is the cathode. Clearly, the in-phase component with an a-c voltage is the same as d-c electroluminescence, and arises from quantum mechanical electron penetration of the cathode barrier followed by acceleration to velocities sufficient for impact excitation of the activator ions.

The out-of-phase component dominates the a-c electroluminescence with low applied voltages. Each pulse is again characteristic of a particular electrode and originates when that electrode is becoming negative during the cycle. Again, the cathode region is the high field region when the electroluminescence occurs. However, the electrons must now originate within the semiconductor. As an electrode goes negative during the voltage cycle, the exhaustion barrier will widen

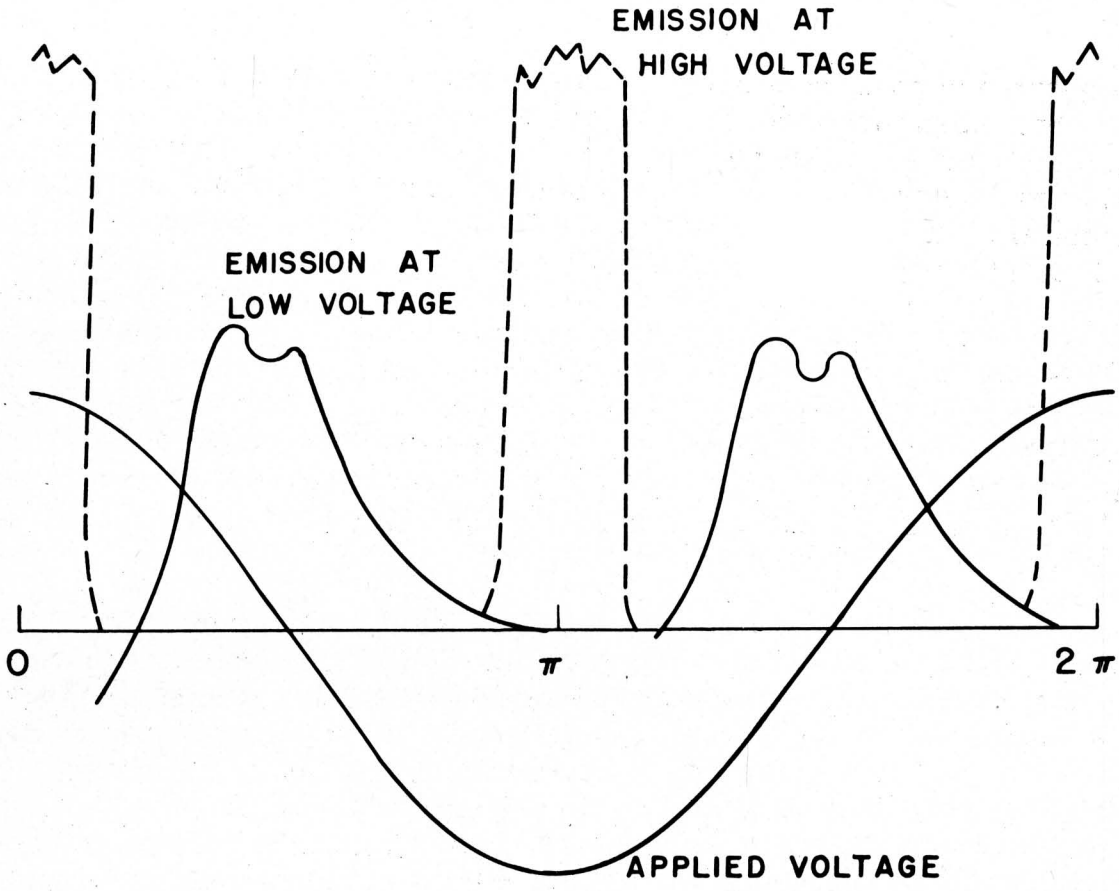

Fig. 15 Phase relationship for ZnS:Cu single crystals of electroluminescent emission and applied voltage--Piper and Williams.(39)

as donor levels are emptied until most of the voltage is across the cathode barrier. An a-c applied voltage depletes and replenishes the barriers at each electrode alternately, as shown in Fig. 16. Deep-lying donor levels will be ionized only by a field which is also sufficient to accelerate electrons. A field of 10^6 v/cm will ionize donor levels 0.5 ev below the conduction band and will accelerate conduction electrons to velocities sufficient for the impact excitation of activator ions.

Independently and concurrently, Curie(43) recognized the relevance of local dielectric breakdown to the electroluminescence of sulfide phosphors.

4. Carrier Injection Mechanism

Lehovec, Accardo, and Jamgochian(44) have made recent investigations on silicon carbide and have proposed that the electroluminescence

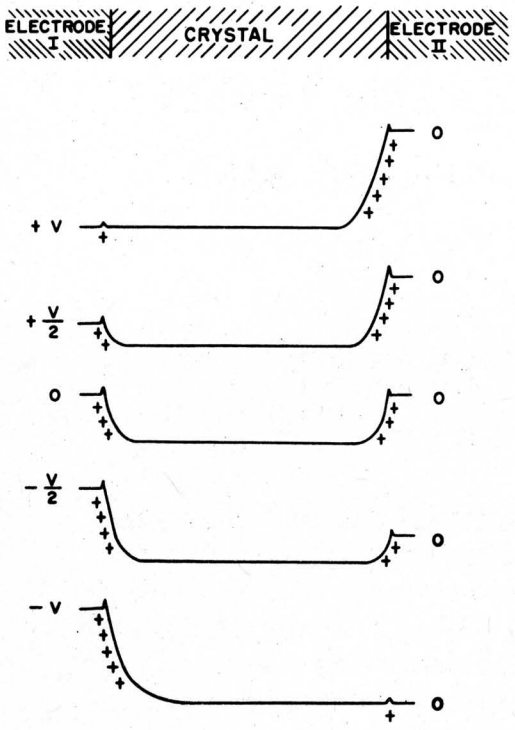

Fig. 16 Band-theory model for changes in barrier layers and donor levels during voltage cycle.

occurs as a result of the optical recombination of charge carriers injected across a barrier layer. Silicon carbide is one of the few substances that is readily prepared as either an N- or a P-type semiconductor. An N-type semiconductor conducts predominantly by negatively charged carriers--electrons in the conduction band; whereas a P-type semiconductor conducts predominantly by positively charged carriers--holes in the filled band. A barrier exists at the junction of an N- and a P-type semiconductor as shown in Fig. 17. With an applied electric field in the direction to urge electrons from the N-type region to the P-type region and holes from the P-type region to the N-type region, current flows easily; whereas with opposite polarity, electrons and holes are exhausted from the contact, a space charge develops, and negligible current flows. With the electric field applied in the direction of easy flow, electrons injected into the P-region recombine with holes and holes injected into the N-region recombine with electrons. The presence of a suitable activator in or near the junction permits the recombination to occur optically with the characteristic emission of the activator. The mechanism is illustrated in Fig. 17. Lehovec, et al., showed that the yellow emission of SiC occurs at P-N junctions when a voltage is applied in the forward direction, and proposed the injection mechanism of electroluminescence.

More recently, Haynes and Briggs[45] have discovered injected electroluminescence in P-N junctions of germanium and silicon. The emission is, of course, in the infrared. They tentatively attribute the emission to direct recombination of an electron at the bottom of the conduction band and a hole at the top of the filled band.

5. Possible Applications of Electroluminescence

Electroluminescence gives promise of application to lighting and electronics. The directness of the conversion in the semiconducting phosphor of electrical energy into visible light suggests that high efficiency

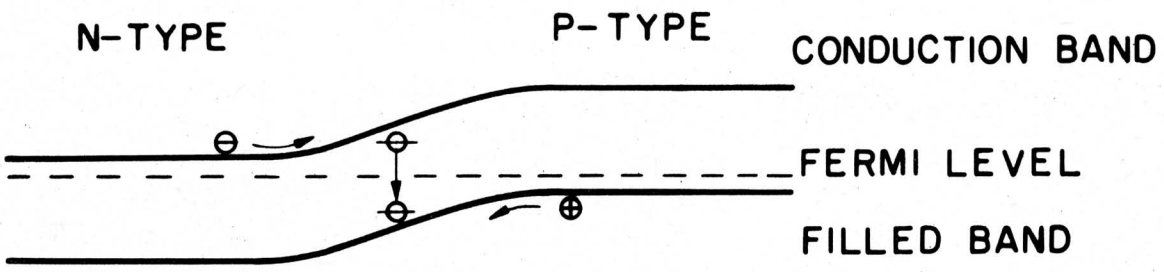

Fig. 17 Band-theory model of carrier injection mechanism for electroluminescence.

may be attainable. So far, however, efficiencies of only a few lumens per watt have been reported. The high frequency response of SiC and the nonlinear characteristic of the in-phase component of ZnS:Cu crystals have obvious applications to electronic devices. In conjunction with crystal detectors, compact optical storage elements are feasible. Most important, the interpretation of the electroluminescence of ZnS:Cu by the impact excitation mechanism and the interpretation of the electroluminescence of SiC by the injection mechanism establish a theoretically sound basis for further fundamental research on electroluminescence.

VI. CATHODE-RAY TUBE SCREENS

1. Contrast and Resolution of Cathode-ray Tube Screens

The conventional cathode-ray tube screen consisting of particles 5 to 15 microns in diameter deposited 10 to 50 microns thick is obviously not an ideal screen for excitation by 10-kv electrons that penetrate only two microns into the phosphor crystals. The resolution is limited by particle size and screen thickness. The local contrast is poor because of scattering and reflection of light from the region excited to adjacent regions. Poor definition and halation rings result. The overall contrast is reduced by the scattering of the ambient illumination, so that the unexcited regions of the screen are not black but only gray. In addition, the brightness of the screen is reduced by absorption of the luminescent emission in traversing the screen thickness, as demonstrated by the greater brightness of the side of the screen on which the electron beam impinges compared with the brightness of the side of the screen which is normally viewed.

The desirability of a continuous, non-grainy transparent phosphor screen for cathode-ray tubes has long been recognized. Theoretically, the feasibility of efficient thin phosphor films is apparent from the

conclusion that the excitation and emission processes are confined to the local environment of the activator ions. However, the preparation of efficient, stable, transparent luminescent films is a quite recent achievement.

2. Evaporated Phosphor Films

The preparation of transparent phosphor films by evaporation of the phosphor or of the phosphor components in a vacuum has been extensively investigated. DeBoer[46] has reported sulfide phosphor screens prepared by evaporation. However, it has subsequently been demonstrated that evaporated zinc sulfide fails to exhibit appreciable luminescence even if a suitable activator is evaporated separately and simultaneously. Heat treatment following condensation improves the luminescence but decreases the transparency by promoting grain growth. Williams[47] showed that manganese-activated zinc fluoride is unique among luminescent materials in being capable of evaporation and condensation in a vacuum to form thin transparent films without unduly affecting the high cathodoluminescent efficiency. Unfortunately, however, fluoride phosphors tend to burn or lose their efficiency under high current densities, and in the form of thin continuous films the tendency is enhanced. Young[48] has been able to convert the unstable evaporated ZnF_2:Mn to stable ZnS:Mn by heating at 500° C in a stream of hydrogen sulfide. Some loss in luminescent efficiency and transparency is experienced, however.

3. Transparent Chemically Deposited Screens

The discovery by Studer and Cusano[48,49] of the chemical deposition technique of depositing phosphor films solved the problem of producing stable, transparent, non-grainy screens of high luminescent efficiency for cathode-ray tubes. This method consists in the formation of the phosphor on a heated surface by the chemical reaction of appropriate vapors. Chemically deposited zinc sulfide containing various activators has been prepared. Zinc vapor plus activator vapor are passed over a glass surface heated to about 550° C in an atmosphere of hydrogen sulfide at a few millimeters of pressure. One arrangement for the process is shown in Fig. 18. The chemical reaction occurs preferentially at the glass surface, and with a properly cleaned surface the zinc sulfide deposits as a clear uniform film, with the activator incorporated so as to give efficient cathodoluminescence. Manganese vaporized with the zinc yields ZnS:Mn, which emits yellow-orange. The use of $ZnCl_2$

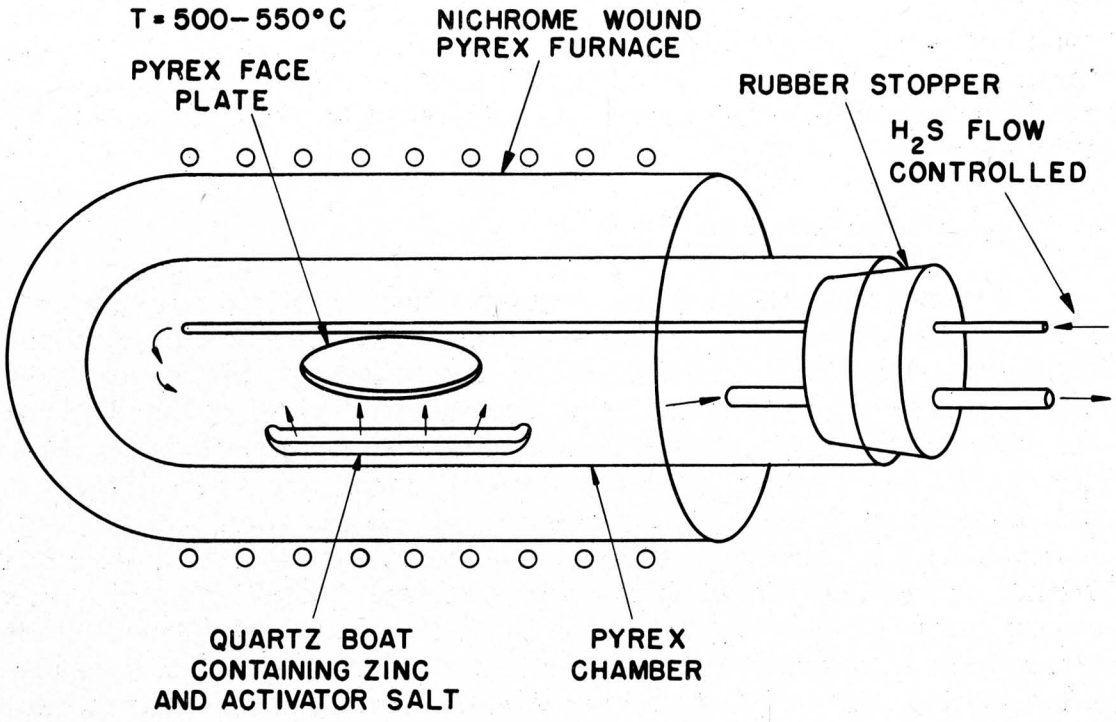

Fig. 18 Apparatus for chemical deposition of transparent phosphor films--Studer, Cusano, and Young.[48]

yields the blue-emitting ZnS:Zn. With double activation, a white-emitting screen having the emission spectrum shown in Fig. 19 is obtained. The spectrum of the present powdered television screen is shown for comparison.

The superior local contrast and resolution of the chemically deposited transparent screen compared to the settled powder screen are shown in the photograph, Fig. 20. Both screens are in the same tube and the focusing of the electron beam is identical in the two cases. The poor definition and halation rings of the powdered screen are obvious. The loss in over-all contrast of powdered screens by the scattering of ambient illumination is shown in Fig. 21 by a photograph of a scanned line on a commercial television tube and on an experimental tube with a chemically deposited transparent screen. Incidentally, the luminescent efficiency of the transparent sulfide film is less than the efficiency of the corresponding powdered phosphor because of internal optical trapping of the light; however, lower brightness does not appear to be a serious limitation because very high brightness is necessary only for screens having very poor contrast characteristics.

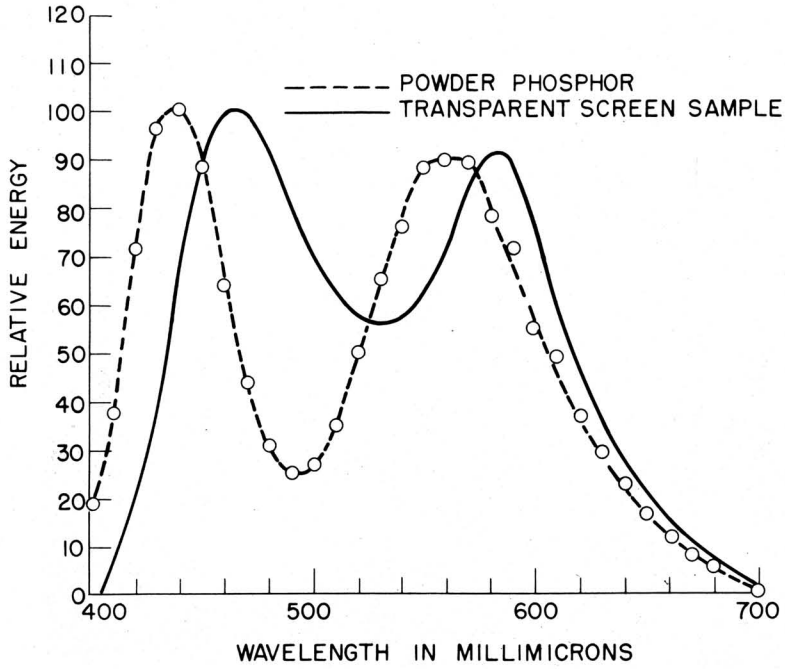

Fig. 19 Emission spectra of transparent and powdered white cathode-ray tube screens.

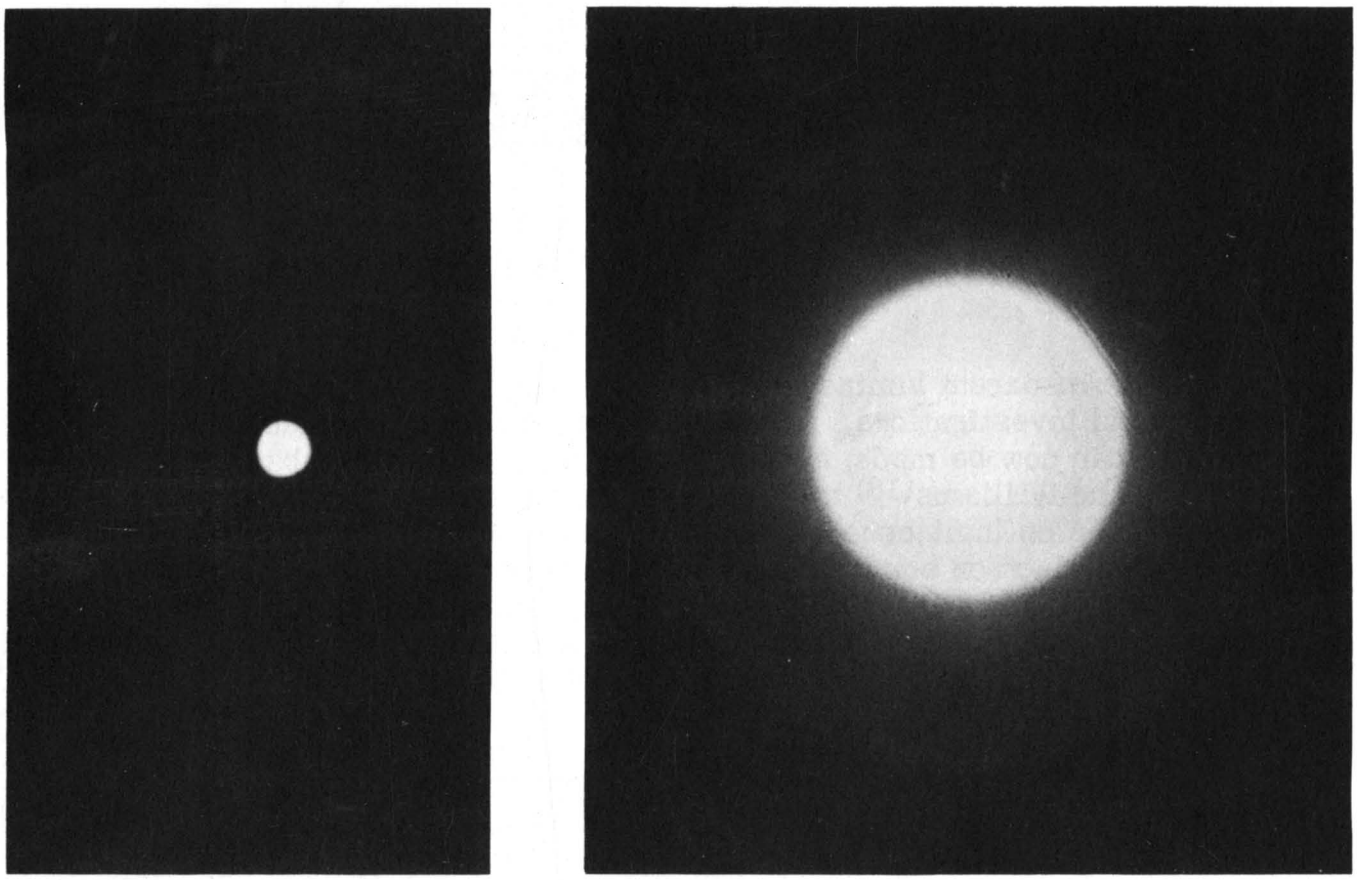

Fig. 20 Electron-beam spot on transparent and powdered cathode-ray tube screens photographed in the dark.

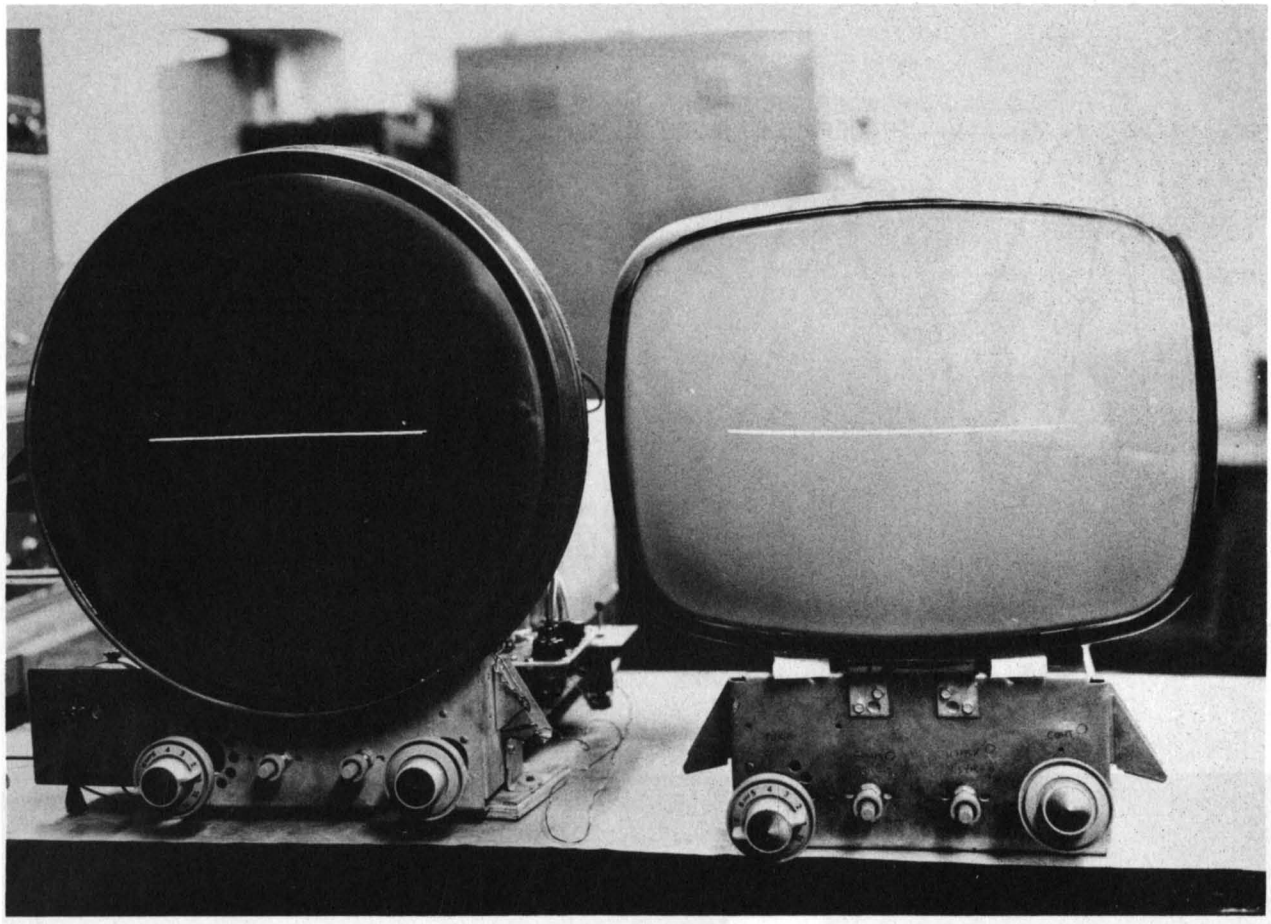

Fig. 21 Scanned line on 16-inch transparent and powdered cathode-ray tube screens photographed with ordinary room illumination.

Transparent luminescent deposits are particularly suitable for many experimental investigations. Absolute optical absorption measurements on phosphors can now be made, even down into the fundamental absorption bands. Parkinson and Williams[18] have reported absorption measurements from 2600 to 1500 A on luminescent ZnF_2:Mn films. Measurements of photoconductivity and electron bombardment enhanced conductivity are feasible with transparent phosphor films. Secondary emission, electron penetration, and electron scattering data on continuous films are more amenable to theoretical interpretation than similar data on powdered phosphors.

4. Energy Loss of Electrons in Penetrating Luminescent Solids

Koller and Alden[50] have recently investigated the energy loss of electrons in penetrating chemically deposited ZnS:Mn films. The films varied in thickness from 0.05 to 1.0 micron and were excited by electron

bombardment in a demountable, post-accelerator cathode-ray tube at voltages up to 30 kv. Aluminum approximately 0.03 micron thick was evaporated on the phosphor film to eliminate sticking. At low voltages, correcting for energy loss in the aluminum, the brightness is linear with the voltage indicating that the luminescent intensity is linear with the energy lost in the phosphor film. This result is in marked contrast with data on powdered phosphors[2] where a complex voltage dependence is observed. At the voltage at which penetration of the phosphor film occurs, departure from linearity is evident and a maximum brightness is approached. Finally, the luminescent emission decreases with increasing voltage at high voltages. A typical experimental curve is shown in Fig. 22.

The well-known theoretical energy loss of an electron in passing through matter, originally derived classically but subsequently confirmed quantum-mechanically, is:

$$V_o^2 - V^2 = bx \quad , \tag{11}$$

where V_o is the initial energy of the incident electron, and V is the energy of the electron after it has traversed a path x. Assuming no scattering, or, in other words, that the path x is equal to the film thickness, the theoretical curve shown in Fig. 22 is obtained from Eq. (11). The pronounced difference in the theoretical and experimental energy-loss functions demonstrates the importance of electron scattering.

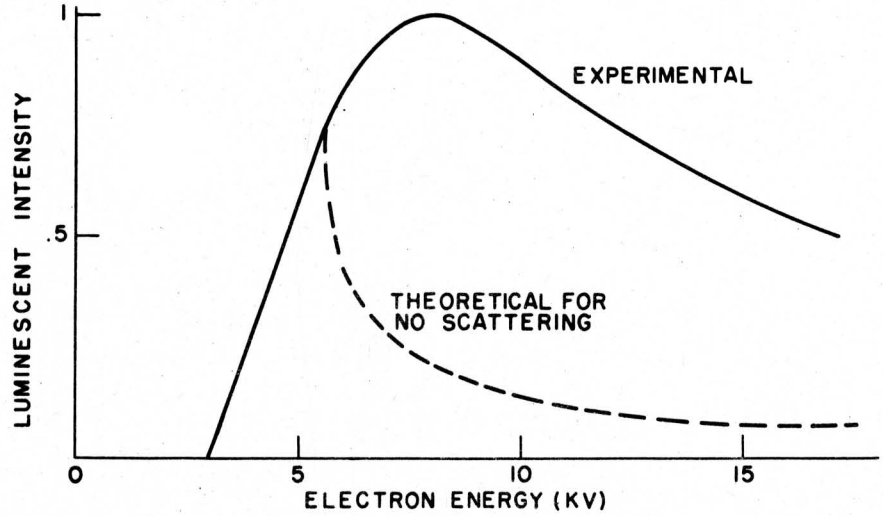

Fig. 22 Experimental and theoretical cathodoluminescent brightness of transparent phosphor films as a function of voltage of the incident electrons.

It is evident, therefore, that transparent phosphor screens are not only a significant advance for cathode-ray tubes in applications where contrast and resolution are important, but also make feasible several crucial experiments in solid-state physics.

ACKNOWLEDGMENTS

The author is indebted to the editors of the Journal of Chemical Physics, the Physical Review, and the Journal of the Optical Society of America, for permission to use the figures reproduced from these journals.

The helpful suggestions of members of the Light Production Studies Section of this laboratory during the preparation of this article are gratefully acknowledged.

REFERENCES

1. Williams, F. E., J. Optical Soc. Am., 39, 648 (1949).

2. Garlick, G. F. J., Advances in Electronics, Vol. II, Academic Press, New York (1950), pp. 151-184.

3. Johnson, P. D., and Williams, F. E., J. Chem. Phys., 18, 1477 (1950).

4. Mayer, J. E., J. Chem. Phys., 1, 270, 327 (1933).

5. Seitz, F., J. Chem. Phys., 6, 150 (1938).

6. Williams, F. E., J. Chem. Phys., 19, 457 (1951).

7. Johnson, P. D., and Williams, F. E., J. Chem. Phys. (in press).

8. Williams, F. E., Phys. Rev., 82, 281L (1951).

9. Williams, F. E., and Hebb, M. H., Phys. Rev., 84, 1181 (1951).

10. Johnson, P. D., and Studer, F. J., Phys. Rev. 82, 976L (1951).

11. Johnson, P. D., and Williams, F. E., J. Chem. Phys., 20, 124 (1952).

12. Hartree, D. R., and Hartree, W., Proc. Roy. Soc. (London), 150, 9 (1935).

13. Randall, J. T., and Wilkins, M. A. F., Proc. Roy. Soc. (London), 184A, 366 (1945).

14. Williams, F. E. (unpublished research).

15. Crawford, J. H., and Williams, F. E., J. Chem. Phys., 18, 775 (1950).

16. Johnson, P. D., and Williams, F. E., J. Chem. Phys., 17, 435 (1949).

17. Johnson, P. D., and Williams, F. E., J. Chem. Phys., 18, 323 (1950).

18. Parkinson, W. W., and Williams, F. E., J. Chem. Phys., 18, 534 (1950).

19. Johnson, J. S., and Williams, F. E., J. Optical Soc. Am., 39, 709 (1949).

20. Kröger, F. A., and Zalm, P., J. Electrochem. Soc., 98, 177 (1951).

21. Tiede, E., and Villain, E., Ber., 73, 274 (1940).

22. Kröger, F. A., Some Aspects of the Luminescence of Solids, Elsevier Publishing Company, New York (1948), p.69.

23. Kröger, F. A., Hoogenstraaten, W., Bottema, M., and Botden, T. P. J., Physica, 14, 81 (1948).

24. Kröger, F. A., and van den Boomgaard, J., J. Electrochem. Soc., 97, 377 (1950).

25. Patten, S. H., and Williams, F. E., J. Optical Soc. Am., 39, 702 (1949).

26. Thorington, L., J. Optical Soc. Am., 40, 579 (1950).

27. Prener, J. S., J. Chem. Phys. (in press).

28. Hershberger, W. D. and Leifer, H. N., Phys. Rev., 88, 714 (1952).

29. Kröger, F. A., Hellingman, J. E., and Smit, N. W., Physica, 15, 990 (1949).

30. Kröger, F. A., and Dikhoff, J., Physica, 16, 297 (1950).

31. Kröger, F. A ., and Smit, N. W., Physica, 16, 317 (1950).

32. Roberts, S., and Williams, F. E., J. Optical Soc. Am., 40, 516 (1950).

33. Wise, M. E., Physica, 17, 1011 (1951).

34. Destriau, G., Phil. Mag., 38, 700 (1947).

35. Payne, E. C., Mager, E. L., and Jerome, C. W., Illum. Eng., 45, 688 (1950).

36. Lossew, O., Phil.Mag., 6, 1028 (1928).

37. Tetzner, H., Z. angew. Phys., 1, (4), 11 (1948).

38. Roberts, S., J. Optical Soc. Am. (in press).

39. Piper, W. W., and Williams, F. E., Phys. Rev., 87, 151L (1952).

40. Piper, W. W., J. Chem. Phys., 20, 1343L (1952).

41. Mott, N. F., Proc. Roy. Soc. (London), 171A, 27 (1939).

42. Schottky, W., Z. Physik, 118, 539 (1942).

43. Curie, D., J. phys. et radium, 13, 317 (1952).

44. Lehovec, K., Accardo, C. A., and Jamgochian, E., Phys. Rev., 83, 603 (1951).

45. Haynes, J. R., and Briggs, H. B., Phys. Rev., 86, 647 (1952).

46. DeBoer, J. H., U.S. Patent 1,954,691 (April 10, 1934).

47. Williams, F. E., J. Optical Soc. Am., 37, 302 (1947).

48. Studer, F. J. Cusano, D. A., and Young, A. H., J. Optical Soc. Am., 41, 559 (1951).

49. Cusano, D. A., and Studer, F. J., Bull. Optical Soc. Am., 37th Annual Meeting, Abstract 58 (1952).

50. Koller, L. R., and Alden, E. D., Phys. Rev., 83, 684L (1951).

DISTRIBUTION LIST

Additional copies of this report will be supplied to qualified persons upon application to:

Research Publication Services
Room 2E3, The Knolls
Schenectady

DEFENSE PRODUCTS GROUP

Aircraft Gas Turbine Division

Lockland, O.
Library

River Works
Accessory Turbine Library

APPARATUS GROUP

Transformer and Allied Products Division

Pittsfield
JH Hagenguth

Turbine Division

X-ray Dept.
Coolidge Lab., Milwaukee
RF Wilson

APPLIANCE AND ELECTRONICS GROUP

Electronics Division

Schenectady
CR Knight
WJ Walker

Syracuse
LT DeVore
Library
C Dichter

FH Ahlburg
PN Russell
LE Record

Major Appliance Division

Bridgeport
RM Lacy
CF Scott

Telechron Department

Ashland, Mass.
AE Miner

INDUSTRIAL PRODUCTS AND LAMP GROUP

Construction Materials Division

Bridgeport
DW Lynch
CH Black

INDUSTRIAL PRODUCTS AND LAMP GROUP (continued)

Lamp Division
Cleveland

HC Froelich, LDL	BT Barnes	G Bogdanoff, LDL
MJ Hamner	DE Elmendorf	R Potter, LDL
WJ Geiger	S McLean	M Weinstein, LDL
CG Found	WF Hodge	Library

Chemical Product Works
1099 Ivanhoe Road, Cleveland 10
WP Cartun (2)

MEASUREMENTS AND INDUSTRIAL PRODUCTS DIVISION
Lighting and Rectifier Department, River Works
HJ Flaherty
EA Harty 2-406

River Works Service Dept.
AC English

ENGINEERING SERVICES DIVISION
Schenectady
J Horn

Technical Data Center
BR Vrooman

Process Technology Program, Technical Education,
Room 194, Building 6, Pittsfield

General Engineering Laboratory
Schenectady
Mrs. FF Buckland

LEGAL AND PATENT SERVICES DIVISION
Patent Services Department
Schenectady
PA Frank

RESEARCH SERVICES DIVISION
Research Laboratory
Schenectady

L. Apker	DA Cusano	CG Fick
EL Brady	R Damon	JC Fisher
JK Bragg	WC Dunlap, Jr.	MD Fiske
DE Chambers	JR Eshbach	VH Fraenckel

RESEARCH SERVICES DIVISION (continued)

Research Laboratory, Schenectady

NT Gordon	RW Larson	S Roberts
RN Hall	JL Lawson	FJ Studer
RE Halsted	HN Leifer	CG Suits
MH Hebb	L Navias	WA Thornton
JD Hoffman	AE Newkirk	WW Tyler
JH Hollomon	MJ Ozeroff	FE Williams (2)
AW Hull	EM Pell	VC Wilson
JP Howe	WW Piper	AH Young
PD Johnson	RS Powell	JR Young
LR Koller	JS Prener	B Zimm
AB Laponsky	RW Redington	Library

KNOLLS ATOMIC POWER LABORATORY

Technical Department

Schenectady

Library

D Van Horn

OTHER

Dr. Gorton R. Fonda
1028 Parkwood Blvd.
Schenectady, N.Y.

GENERAL ELECTRIC

Research Laboratory

SCHENECTADY, N. Y.